Geological Society of America Special Papers Online First

Early Cretaceous to present latitude of the central proto-Tibetan Plateau: A paleomagnetic synthesis with implications for Cenozoic tectonics, paleogeography, and climate of Asia

Peter C. Lippert, Douwe J.J. van Hinsbergen and Guillaume Dupont-Nivet

E-mail alerting services	click www.gsapubs.org/cgi/alerts to receive free e-mail alerts when new articles cite this article
Subscribe	click www.gsapubs.org/subscriptions to subscribe to Geological Society of America Special Papers
Permission request	click www.geosociety.org/pubs/copyrt.htm#gsa to contact GSA.

Notes

THE
GEOLOGICAL
SOCIETY
OF AMERICA

Early Cretaceous to present latitude of the central proto-Tibetan Plateau: A paleomagnetic synthesis with implications for Cenozoic tectonics, paleogeography, and climate of Asia

Peter C. Lippert*

Department of Geosciences, University of Arizona, Tucson, Arizona 85721, USA

Douwe J.J. van Hinsbergen

Department of Earth Sciences, University of Utrecht, Budapestlaan 4, 3584 CD Utrecht, Netherlands

Guillaume Dupont-Nivet

*Géosciences Rennes, Unités Mixte de Recherche 6118, Université de Rennes 1,
Campus de Beaulieu, 35042 Rennes Cedex, France*

*Palaeomagnetic Laboratory Fort Hoofddijk, Department of Earth Sciences,
University of Utrecht, Budapestlaan 17, 3584 CD Utrecht, Netherlands*

*Key Laboratory of Orogenic Belts and Crustal Evolution,
Ministry of Education, Peking University, Beijing 100871, China*

ABSTRACT

Published paleomagnetic data from well-dated sedimentary rocks and lavas from the Lhasa terrane have been reevaluated in a statistically consistent framework to assess the latitude history of southern Tibet from ca. 110 Ma to the present. The resulting apparent polar wander path shows that the margin of the Lhasa terrane has remained at lat ~20° ± 4°N from ca. 110 to at least 50 Ma and has drifted northward to its present latitude of 29°N since the early Eocene. This latitude history provides a paleomagnetically determined collision age between the Tibetan Himalaya and the southern margin of Asia that is ca. 49.5 ± 4.5 Ma, if not a few millions of years earlier after considering reasonable estimates for shortening within the suture zone. This collision occurred at lat ~21° ± 4°N, or perhaps ~2° lower if an average-size forearc is considered. These paleomagnetic data indicate that at most, only 1100 ± 560 km of post–50 Ma India-Asia convergence was partitioned into Asian lithosphere. The lower bound of these paleomagnetic estimates is consistent with the magnitude of upper crustal shortening and thickening within Asia calculated from structural geologic studies. Thus, a substantial amount of the shortening within, and therefore surface uplift of, the Tibetan Plateau predates the Tibetan Himalaya–Lhasa collision. These conclusions suggest that the Tibetan Plateau is similar to the Altiplano of the Andes,

*plippert@email.arizona.edu

in that most of the plateau developed at subtropical latitudes above an oceanic subduction zone in the absence of a continent-continent collision. A direct implication of these findings is that 1700 ± 560 km or more post–50 Ma India-Asia convergence was partitioned into the lower plate of the orogenic system (i.e., units of Indian affinity). Recent paleomagnetic and plate tectonic analyses suggested significant extension of Greater India lithosphere after breakup from Gondwana but prior to collision with the southern margin of Asia. Cretaceous extension within Greater India was inferred to open an oceanic Greater India Basin, which would have maintained a deep tropical water mass along the southern edge of greater Asia throughout most of the Paleogene. We suggest ways in which future climate models can incorporate this paleogeography to more accurately explore how Paleogene atmospheric processes interact with or are modified by the juxtaposition of a tropical ocean basin and the high uniform topography of the Tibetan Plateau.

INTRODUCTION

The thick crust and elevated, low relief surfaces of orogenic plateaus such as the Altiplano in the Andes, the Turkish-Iranian high plateau, or the Tibetan Plateau are among the most conspicuous physiographic features on Earth. These first-order attributes of plateaus have motivated considerable research exploring possible feedbacks between plateau growth and plate force balances (e.g., for Tibet, Molnar and Lyon-Caen, 1988; Flesch et al., 2005; Iaffaldano et al., 2007; Molnar and Stock, 2009; Copley et al., 2010, 2011; for the Andes, Oncken et al., 2006; for the Turkish-Iranian plateau, Allen et al., 2004; Sengör et al., 2008), as well as potential feedbacks between plateau growth and atmospheric dynamics and related climate evolution (e.g., Manabe and Terpstra, 1974; Sobel et al., 2003; see review in Molnar et al., 2010). In general, plateaus result from distributed compressional deformation at leading edges of overriding continental plates above subduction zones, followed, in places, by continent-continent collision. The Tibetan Plateau is an ideal case study for understanding partitioning of strain related to India-Asia convergence into the overriding Asian plate since the Early Cretaceous, first during oceanic subduction and subsequently during continent-continent collision stages (Murphy et al., 1997; DeCelles et al., 2007; Kapp et al., 2007a, 2007b; Rohrmann et al., 2012). This strain is now manifested as the modern Tibetan Plateau, which creates a barrier to west-to-east subtropical tropospheric air flow and seasonally pulls the Intertropical Convergence Zone (ITCZ) far north of the equator. These perturbations to atmospheric circulation affect not just the regional climate of Asia, but also possibly the global distribution of heat and moisture (see reviews in Rodwell and Hoskins, 1996; Molnar et al., 2010; Huber and Goldner, 2012). The plateau and high Himalaya also prevent cool, dry subtropical air from Central Asia from mixing with warm, humid tropical air from the Indian Ocean, and therefore may simultaneously accentuate the Indian monsoon and the subtropical aridity that characterizes the climate of western China and surrounding regions (Boos and Kuang, 2010).

Similar processes probably have been active since the plateau first reached an as-yet unknown critical extent and height,

but the response of atmospheric dynamics and feedbacks with surface processes to the presence of a Tibetan Plateau also may be sensitive to its latitudinal position (e.g., within the arid subtropics; Sobel et al., 2003). Thus, climate models that explore the role of the Tibetan Plateau in regional climate change should evaluate the distribution of high-elevation, low-relief topography not only in time, but also in (latitudinal) space. A key first step in addressing any of these relationships is to quantitatively constrain the paleogeography of the Tibetan Plateau throughout its geologic history in terms of its surface uplift, its structural position relative to Eurasia and India, and its latitude. In this paper we address the latter history using paleomagnetism. The convergence between India and Asia is essentially north-south, and positions of the Indian and Asian continents are reconstructed in detail based on marine magnetic anomalies (e.g., Molnar and Stock, 2009; Copley et al., 2010; Cande and Stegman, 2011; van Hinsbergen et al., 2011b). Paleomagnetic data, and paleolatitudinal motion derived from inclination values, are thus very useful tools to date collisional events from rocks of the deformed northern Indian and southern Eurasian margin, and can quantify how convergence is partitioned into strain in the upper and lower plates of the orogen (Besse et al., 1984; Chen et al., 1993; Dupont-Nivet et al., 2010a; Lippert et al., 2011; van Hinsbergen et al., 2012b).

Several recent paleomagnetic studies of volcanic and sedimentary units of Cretaceous to Paleogene age from the Lhasa terrane allow us to construct a detailed paleolatitude record for southern Tibet. The results from these studies are highly variable, however, and have been used at face value to support disparate paleogeographic reconstructions. For example, Achache et al. (1984), Tan et al. (2010), Dupont-Nivet et al. (2010a), Liebke et al. (2010), Sun et al. (2010), and Chen et al. (2010) each sampled the upper Linzizong Formation (Pana formation of Liu, 1993), which consists of felsic volcanic rocks and interlayered terrestrial sediments and is widely distributed across the southern Lhasa terrane, and has been well dated to 57–46 Ma using both $^{40}Ar/^{39}Ar$ (Lee et al., 2009) and U-Pb (He et al., 2007) isotopic systems. Calculated paleolatitudes range from 8°N (Chen et al., 2010) to 33°N (Tan et al., 2010). It is not possible for all of these individual paleolatitude estimates to be accurate within such a short time interval.

The purpose of this study is to utilize the wealth of new paleomagnetic data from the Lhasa terrane to produce a robust paleolatitude history of the southern margin of the Tibetan Plateau. We accomplish this by combining and interpreting time-equivalent paleomagnetic data in a coherent and statistically equivalent framework. Previous reviews of paleomagnetic data from the Lhasa terrane (e.g., Ali and Aitchison, 2006; Liebke et al., 2010; Najman et al., 2010) have treated published averaged paleomagnetic data with equal statistical weight even though these averaged data are disparate in terms of sample size and underlying selection criteria. Herein we demonstrate why this approach should be used with caution in the context of the India-Asia collision. Our approach is strictly a statistical one, with an emphasis on applying the same methodology to each data set to establish coherency within and between paleomagnetic data sets from southern Tibet. Our synthetic approach should provide data sets that are large enough and varied enough in sampling strategy to perform statistically robust and geologically meaningful paleomagnetic field tests and tests for averaging of paleosecular variation in the cases involving volcanic units. Our approach should also help identify the source or cause of the variability between the results from individual paleomagnetic studies, indicate sampling gaps in the paleomagnetic record, and provide a latitude history for southern Tibet that can be tested by future research. This information is crucial for designing sampling strategies for field campaigns that will maximize the utility, quality, and robustness of future paleomagnetic studies of the Lhasa terrane.

We summarize the published paleomagnetic data from Cretaceous to Paleogene stratigraphic units from the Lhasa terrane and then evaluate these data for consistent quality using the most up-to-date criteria achieved by the geomagnetic field community. This study is an update of paleomagnetic data presented in van Hinsbergen et al. (2012b, their supplementary information), and here is discussed specifically in the context of the Lhasa terrane and Tibetan Plateau. We discuss these results in terms of calculating the paleolatitude for the southern margin of Asia since ca. 110 Ma. We conclude with a brief discussion of implications for the Cenozoic tectonics of the India-Asia collision and Tibetan Plateau and regional climate dynamics; we also highlight potential directions for future research.

METHODS: PALEOMAGNETIC ARCHIVES OF LATITUDE

Global Synthetic Apparent Polar Wander Path and Kinematic Plate Reconstructions: Positioning India and Asia

The relative positions of plates that are bounded by active or former mid-ocean ridges are determined by plate circuits based on marine magnetic anomalies and fracture zones (Cox and Hart, 1986). The position of the plate circuit is constrained relative to the dipolar geomagnetic field assumed to parallel the Earth's spin axis in a so-called global apparent polar wander path

(GAPWP), which utilizes paleomagnetic data from the stable continents. Here we use the most recent GAPWP of Torsvik et al. (2012), which was constructed by first rotating all available high-quality paleomagnetic poles from each stable continental region to a common reference location (e.g., South African plate) using the Euler poles from the plate circuit, then time-averaging these paleomagnetic data, and finally transforming this smoothed paleomagnetic pole path back to each continental reference frame using the same plate circuit.

The GAPWP provides paleolatitudes to within a few degrees uncertainty, because the synthetic nature and long-time averaging of synthetic GAPWPs reduce uncertainties and introduce some smoothing in the position of the mean apparent paleomagnetic pole for a continental block (for a review, see Torsvik et al., 2012). It is important to note that some Paleogene paleomagnetic data from Central and East Asia yield anomalously low paleolatitudes relative to the global database (e.g., Si and van der Voo, 2001; Cogné et al., 1999, 2013; Dupont-Nivet et al., 2010b; Lippert et al., 2011). These data were omitted from the GAPWP compilation of Torsvik et al. (2012). The GAPWP provides precise positions of stable Siberia-Eurasia and India.

Despite their precision, plate circuits provide only relative positions and motions of one plate relative to another, and the GAPWP provides precise locations only of the stable regions of continents relative to the spin axis. Relics of former plates such as the Tibetan microcontinental fragments or intensely deformed Indian and Asian plate boundaries cannot be directly reconstructed in a plate circuit and GAPWP, contrary to some interpretations (Ali and Aitchison, 2004, 2006; Aitchison et al., 2007). The only way to quantitatively place such regions, including Tibet, into past plate paleogeographic configurations is by using paleomagnetic data, constraining paleolatitude and vertical axis rotation (but not paleolongitude). Thus, placing highly deformed regions like southern Tibet within the context of the global plate circuit, i.e., quantifying the paleogeography of orogens in space and time, requires paleomagnetic data from the orogen. The paleolatitudes of deformed continental margins like the northern edge of Greater India and the southern edge of the Tibetan orogen, i.e., zero-order paleogeographic boundary conditions for calculating continental collision events, the distribution of strain within the orogen, and feedbacks between topography, atmospheric dynamics, and climate, must be calculated from robust paleomagnetic data from the margins (e.g., Dupont-Nivet et al., 2010a; Yi et al., 2011).

Positioning Tibet within India-Asia Convergence

Data Selection

A robust paleomagnetic pole is calculated from primary, well-dated, well-determined, independent readings of the geomagnetic field over a time period that is long enough to average the effect of secular variation, but short enough so as to not integrate significant plate motion (e.g., van der Voo, 1990). This record can come from sedimentary rocks and lavas, although evaluating the fidelity of this record is very different for the two media. It is generally

assumed that continuous sections of sedimentary rocks naturally average secular variation, such that a stratigraphic series of site mean directions or a magnetostratigraphic column will provide a good characterization of the magnetic field. This assumption is only valid, however, if the preserved magnetic directions are primary and have not been biased by sedimentary inclination shallowing caused by particle settling and compaction (King, 1955). Sedimentary inclination shallowing is especially prevalent in detrital rocks (Lovlie and Torsvik, 1984; Tauxe and Kent, 2004; Kodama, 2009) and is well documented throughout Asia (e.g., Gilder et al., 2001; Yan et al., 2005; see also recent reviews in Dupont-Nivet et al., 2010b; Lippert et al., 2011). Therefore, paleomagnetic results from sediments should be used for paleolatitude reconstructions only after they have been evaluated for this inclination shallowing bias. The likelihood that a sedimentary paleomagnetic data set represents a time-averaged geomagnetic field direction can be evaluated with reasonable assumptions about geomagnetic field behavior (Deenen et al., 2011).

In principle, volcanic rocks are immune to the inclination shallowing bias that appears prevalent in many detrital rocks. Because the processes and time scales by which and over which magnetic directions are recorded in volcanic rocks are fundamentally different from those in sediments, using the paleomagnetism of lavas for tectonic investigations poses unique sampling requirements. Cooling of a single, thin (1–3 m) lava unit will record a geologically instantaneous measurement of the geomagnetic field (~3–30 days; Turcotte and Schubert, 2002). Furthermore, lavas can extrude rapidly as well as irregularly, such that several stratigraphically successive lavas often record the same magnetic field direction. Therefore, paleomagnetic data from volcanic units should first be filtered so that all site mean directions are of comparably high statistical quality, and then, if the sampling strategy permits, stratigraphically successive site mean directions that are statistically indistinguishable should be combined into direction groups (e.g., Mankinen et al., 1985). This procedure ensures that several independent readings of the geomagnetic field have been sampled to accurately characterize its time-averaged behavior and direction.

In this study, we apply the following filtering criteria to site mean directions determined from lavas by excluding sites that (1) are not used by the original authors if reason for exclusion is provided; (2) contain directions of mixed polarity, as lava sites should be spot readings that cannot record a reversal; (3) are characterized by fewer than five samples; (4) have k-values (Fisher's [1953] precision parameter) <50; or (5) or are beyond the angular threshold determined by the Vandamme (1994) cut-off criteria.

This filtering procedure is commonly used by the geomagnetic field community (Johnson et al., 2008), but we note that this treatment of volcanic-based paleomagnetic data is seldom employed in the tectonics community.

Data Processing

Paleomagnetic studies of the present and ancient magnetic field indicate that virtual geomagnetic poles (VGPs) fit a Fisherian distribution better than the parent directions (e.g., Johnson et al., 2008). Therefore, we transform paleomagnetic directions into VGPs and calculate the Fisher mean VGP for each sampling locality. We note that use of the Vandamme (1994) cut-off criteria or a fixed 45° angular cut-off for identifying directional outliers provides the same results for the data sets examined in the following. The assignment of direction groups follows from the original authors of each of the studies. We evaluate the likelihood that a mean lava-based VGP represents the time-averaged geomagnetic field following Deenen et al. (2011). If the calculated error (A95) of the mean VGP is within the error envelope that can be expected based on paleosecular variation models, expressed as $A95_{min}$ and $A95_{max}$ (minimum and maximum), then we conclude that the mean VGP is a time-averaged paleomagnetic pole suitable for paleogeographic studies.

This approach is similar to testing if the angular dispersion (S) of VGPs is similar to the dispersion observed in ancient lavas that yield good estimates of a geocentric axial dipole (GAD) field when averaged (Biggin et al., 2008; Johnson et al., 2008) and to the dispersion determined from paleosecular variation models like TK03.GAD (Tauxe and Kent, 2004). Although the use of S for evaluating time averaging of secular variation has been disputed (Linder and Gilder, 2012), we contend that direct comparison of the directional distributions of ancient lava-based paleomagnetic data to those of large sets of recent lava-based paleomagnetic data (in contrast to comparisons to numerical models or sedimentary data) is the most reasonable approach. Notably, if the angular dispersion of the VGPs is consistent with dispersion observed in young lava successions, then we conclude that the sample set characterizes the time-averaged geomagnetic field.

To determine the Cretaceous–Paleogene latitude of the southern margin of the Lhasa terrane, we calculate the expected paleolatitude and its uncertainty at a reference location on the Indus-Yarlung suture zone (IYSZ, 29°N, 88°E) from each accepted paleomagnetic pole using equations provided in Butler (1992). Until the ca. 55–50 Ma arrival of the Tibetan Himalaya in the subduction zone below Tibet, the southern margin of Asia was located along the modern IYSZ that generally separates rocks of Asian affinity from those of Tibetan Himalayan affinity (IYSZ, Fig. 1) (Hodges, 2000; Hébert et al., 2012). Tibetan Himalayan upper crustal rocks subsequently accreted to and deformed southern Asia, and the southern margin of Asia consequently migrated south of the IYSZ (van Hinsbergen et al., 2012a, 2012b). To keep the same reference point through time, we identify the location of the southern Asian plate boundary until 50 Ma, and the Indus-Yarlung suture thereafter. All calculations are made assuming a 100% axial dipolar geomagnetic field (cf. Si and van der Voo, 2001; Dupont-Nivet et al., 2010b). Paleomagnetic poles and paleolatitudes are listed in Table 1. All age assignments follow the original authors unless otherwise noted and are keyed to the same time scales as used in the global synthetic GAPWP and kinematic plate reconstructions (Torsvik et al., 2012); i.e., Gradstein et al. (1994) for the Mesozoic, and Cande and Kent (1995) for the Late Cretaceous and younger, unless the section is dated using isotopic age determinations.
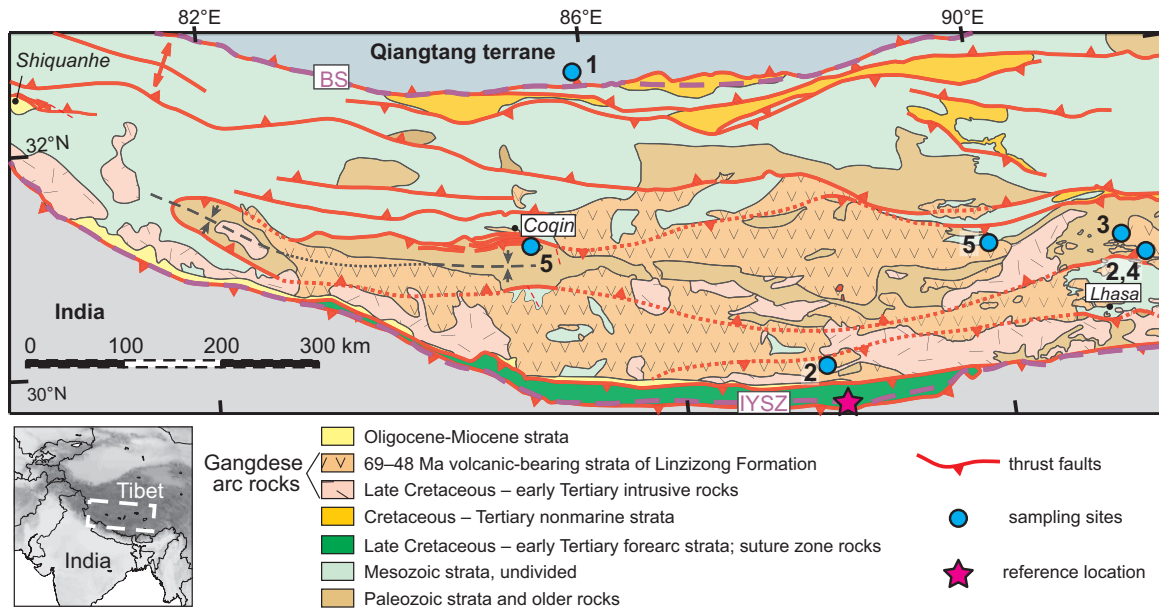
Figure 1. Tectonostratigraphic map of the central Lhasa terrane, southern Tibet (modified by Kapp et al., 2007b). Numbers next to blue circles correspond to locations of paleomagnetic sampling sites discussed in the text. 1—Eocene–Oligocene lavas from the southern Qiangtang terrane; 2—late Eocene lavas and tuffs of the Linzizong Formation; 3—late Cretaceous redbeds of the Shexing Formation; 4—upper Cretaceous redbeds of the Takena Formation; 5—early Cretaceous lavas of the Woronggou Formation and Zenong Group. IYSZ—Indus-Yarlung suture zone. Lower left inset is shaded relief map of central Asia, showing the distribution of high elevation (darker shades) and political boundaries.

PALEOMAGNETIC DATA FROM THE LHASA TERRANE

Eocene–Oligocene Lavas

Paleomagnetic data from late Eocene–early Oligocene (35 ± 3 Ma) basaltic lavas from the Qiangtang block were reported in Lippert et al. (2011). These lavas have been well dated using step-heating $^{40}Ar/^{39}Ar$ methods on bulk rock samples and hornblende or sanidine separates (Ding et al., 2007; Lippert et al., 2011). Site mean directions (n = 33) from three sampling localities have been filtered and binned into 20 statistically independent direction groups; the angular dispersion of the corresponding VGPs is consistent with modern secular variation studies. These lavas yield a maximum likelihood estimate of paleolatitude of 28.7° ± 3.7°N at a present reference site at 33°N, 88°E on the Lhasa-Qiangtang suture. Because there was negligible north-south–directed upper crustal shortening within the Lhasa block throughout the Neogene (Kapp et al., 2005, 2007a, 2007b; Volkmer et al., 2007; Pullen et al., 2008; Rohrmann et al., 2012), we can transfer this paleolatitude directly to our reference position on the IYSZ, 4° of latitude to the south. This results in a paleolatitude estimate for the reference location on the southern margin of Asia of 24.7° ± 3.8°N at 35 ± 3 Ma.

Paleogene Lavas: The Linzizong Formation

Basaltic to andesitic lavas, felsic tuffs, and volcaniclastic units of the Paleocene to early Eocene (64–47 Ma) Linzizong Formation blanket a large area of the southern Lhasa block (Fig. 1)

(He et al., 2007; Lee et al., 2009). The Linzizong Formation is the extrusive component of the Cenozoic part of the Gangdese magmatic arc (Mo et al., 2008), and it is variably divided into three (Dianzhong, Nianbo, Pana; Liu, 1993) or four (K-T, T1, T2, T3; He et al., 2007) subunits distinguished by petrology and unconformities. Although paleomagnetic data have been collected from all members of the Linzizong Formation (e.g., Chen et al., 2010), unfortunately too few published site mean directions from the lower and uppermost members meet our quality criteria to allow further consideration here (although, see Huang et al., 2013). Moreover, it is likely that sedimentary units below the T2 (He et al., 2007) and Pana Formation (Liu, 1993) have been remagnetized or have been affected by syndepositional and postdepositional inclination shallowing; the latter is almost certainly true for sedimentary units above the T2-Pana Formation (Huang et al., 2013). Here we only use paleomagnetic results from the felsic welded tuffs of the Pana unit (Liu, 1993) (unit T2 of He et al., 2007). This volcanic sequence is well dated as ca. 56–47 Ma using both whole-rock $^{40}Ar/^{39}Ar$ (Lee et al., 2009) and zircon U/Pb (He et al., 2007) isotopic methods. Paleomagnetic data compiled in this study were collected from several separate localities of Linzizong Formation outcrops, but all are within ~200 km of the city of Lhasa (Fig. 1). Although Chinese geophysicists conducted paleomagnetic investigations of the Linzizong Formation from the early 1980s (e.g., Zhu et al., 1981), Achache et al. (1984) provided the first paleomagnetic results from the Linzizong Formation described in the English-language literature. Achache et al. (1984) sampled the Linzizong Formation along the Lhasa-Golmud highway between

TABLE 1. PALEOMAGNETIC POLES USED IN THIS STUDY

Figures 1 and 5	Location	Stratigraphic age	Age (Ma)	N (N, n)	Pole latitude (°N)	Pole longitude (°E)	A95	K	S	A95min	A95max	Ip	±	ΔIp	Source
Southern Lhasa block															
1	South Qiangtang	Eocene–Oligocene	35 ± 3	20	—	—	—	—	—	—	—	24.7	±	3.8	a
2	Penbo	Paleocene–Eocene	51.5 ± 4.5	41	80.2	230.4	4.1	30.5	14.8	3.3	6.1	21.1	±	4.1	b
3	Maxiang	Upper Cretaceous	86 ± 14	100	74.6	346.5	2.7	—	—	2.7	4.5	24.9	±	2.7	c
4	Penbo	Upper Cretaceous	97 ± 7	377	79.6	329.9	2.2	—	—	1.6	2.0	23.7	±	2.2	d
5	Deqing and Cuoqin	Lower Cretaceous	120 ± 10	13	—	—	—	—	—	—	—	16.2	±	3.6	e, f
Tibetan Himalaya															
6	Zongpu	Selandian–Thanetian	59 ± 3	243	69.6	272.5	1.7	—	—	1.9	2.6	8.7	±	1.7	g, h
7	Zongshan	Campanian–Maastrichtian	68 ± 3	144	55.8	261.6	3.5	—	—	2.3	3.6	−5.0	±	3.5	g
Indian APWP															
			0	24	88.5	173.9	1.9	—	—	—	—	29.1	±	1.9	—
			10	49	87.2	240.4	1.8	—	—	—	—	26.5	±	1.8	—
			20	31	83.7	254.7	2.6	—	—	—	—	22.9	±	2.6	—
			30	24	79.7	281.7	2.6	—	—	—	—	19.0	±	2.6	—
			40	24	74.7	286.8	2.9	—	—	—	—	14.4	±	2.9	—
			50	33	65.1	278.4	2.8	—	—	—	—	4.4	±	2.8	—
			60	44	48.5	280.8	2.1	—	—	—	—	−11.7	±	2.1	—
			70	32	36.4	280.7	2.5	—	—	—	—	−23.5	±	2.5	—
			80	25	29.0	283.5	2.9	—	—	—	—	−30.1	±	2.9	—
			90	28	20.9	291.4	2.5	—	—	—	—	−35.2	±	2.5	—
			100	14	19.7	293.0	3.3	—	—	—	—	−35.7	±	3.3	—
			110	21	11.1	295.9	3.3	—	—	—	—	−41.7	±	3.3	—
			120	28	8.6	296.4	2.6	—	—	—	—	−43.5	±	2.6	—
			130	18	−1.0	297.1	2.8	—	—	—	—	−50.6	±	2.8	—
Asian APWP															
			0	24	88.5	173.9	1.9	—	—	—	—	29.1	±	1.9	—
			10	49	86.7	150.0	1.8	—	—	—	—	30.5	±	1.8	—
			20	31	84.4	152.1	2.6	—	—	—	—	31.3	±	2.6	—
			30	24	83.1	146.5	2.6	—	—	—	—	32.4	±	2.6	—
			40	24	81.1	144.3	2.9	—	—	—	—	33.6	±	2.9	—
			50	33	78.9	164.7	2.8	—	—	—	—	31.0	±	2.8	—
			60	44	78.2	172.6	2.1	—	—	—	—	29.4	±	2.1	—
			70	32	79.2	175.7	2.5	—	—	—	—	28.9	±	2.5	—
			80	25	79.7	177.9	2.9	—	—	—	—	28.5	±	2.9	—
			90	28	80.4	167.2	2.5	—	—	—	—	30.4	±	2.5	—
			100	14	80.8	152.3	3.3	—	—	—	—	32.6	±	3.3	—
			110	21	81.2	193.1	3.3	—	—	—	—	26.4	±	3.3	—
			120	28	79.0	190.1	2.6	—	—	—	—	26.2	±	2.6	—
			130	18	75.0	183.4	2.8	—	—	—	—	26.6	±	2.8	—

Note: APWP—apparent polar wander path. Location—region from which paleomagnetic data were collected. **N** (N, *n*)—the number of paleomagnetic poles, virtual geomagnetic poles (VGPs), or samples used to calculate the mean paleomagnetic poles listed in this table. A95—the radius of the 95% confidence cone on the mean pole; when calculated from samples rather than poles of VGPs, A95 = $(dp*dm)$^0.5, where *dp* and *dm* are the axes of the oval of 95% confidence about the mean pole calculated from the population of samples. K—the Fisher precision parameter of the mean pole. S—the dispersion of the VGP population. A95$_{min}$/$_{max}$—the minimum and maximum values of A95 given N that the sampled population of paleomagnetic data averages secular variation (Deenen et al., 2011). A dash (hyphen) indicates parameter is not applicable to this data set. I$_p$ ± ΔI$_p$—paleolatitude and 95% confidence interval for a reference site at 29°N, 88°E from pole; calculations follow Butler (1992). Sources: a—Lippert et al. (2011); b—this study (see text and Table 2 for specific studies) with ages from He et al. (2007) and Lee et al. (2009); c—Sun et al. (2011); d—Tan et al. (2010); e—Sun et al. (2008); f—Chen et al. (2011); g—Patzelt et al. (1996) and Dupont-Nivet et al. (2010a); h—Yi et al. (2011); i—table 11 of Torsvik et al. (2012).

Lhasa and Yangbajing, as well as near Linzhou, ~50 km northeast of Lhasa. Most subsequent paleomagnetic studies have concentrated on the exceptional exposures of the Linzizong Formation at Linzhou (Chen et al., 2010; Dupont-Nivet et al., 2010a; Liebke et al., 2010; Tan et al., 2010). A more regional picture is now available, however, with results from Mendui, ~25 km west-northwest of Linzhou (Sun et al., 2010), and from the Namling Basin near Shigatse, ~225 km southwest of Lhasa (Chen et al., 2010) (Fig. 1). The reported paleolatitude estimates for the reference location on the IYSZ from these individual studies range from ~8°N to as high as ~33°N, and these different estimates have been used to construct disparate tectonic models for the India-Asia collision and Tibetan Plateau. One of the goals of this study is to identify the source of this variability in these paleomagnetic data. We hypothesize that it is primarily the result of the low number (e.g., ~10) of independent site mean directions of high statistical quality acquired in each study.

Our compilation of reliable results includes five studies of the upper Linzizong Formation (i.e., T2–Pana Formation) listed in Table A1 in the GSA Data Repository[1] and shown in Figure 2. We have explicitly excluded other historical paleomagnetic studies of the Linzizong Formation (e.g., Pozzi et al., 1982; Westphal and Pozzi, 1983) because these reports have very small numbers of site mean directions, and because the more recent studies noted supersede all of these previous studies in terms of overall data quality and geomagnetic field representation. (For detailed rock magnetism and paleomagnetism of Linzizong Formation units sampled in each study, see the original publications; here we summarize the most salient observations.)

The magnetism of the T2–Pana member of the Linzizong Formation volcanic units is typically carried by magnetite to low-titanium titanomagnetite with some high-titanium titanomagnetite or maghemite. These units often display two components of magnetization in orthogonal vector plots. A low-coercivity or low-temperature direction is indistinguishable from the modern field direction in in situ coordinates and is interpreted to record a viscous overprint. A higher coercivity or high-temperature direction that is distinct from the lower treatment level direction and shows univectoral decay toward the origin over several (>5) consecutive treatment steps on orthogonal vector plots defines the characteristic remanent magnetization (ChRM). In cases where maghemite has been detected, the low and high treatment level directions are not as distinct and the ChRM is determined using great circle direction fits (Dupont-Nivet et al., 2010a; Liebke et al., 2010). The tilt-corrected ChRM is often interpreted to be the primary remanent magnetization, although for most studies, the sampling strategy, results, or a combination of both preclude a rigorous paleomagnetic field test to clearly demonstrate this primary nature. Site mean directions from each study are presented

in Table A1 (see footnote 1), and the mean VGPs and the corresponding latitude of the southern margin of the Lhasa block, at 29°N, 88°E, calculated from these poles are presented in Table 2.

There is considerable variation in not just the calculated paleolatitudes, as described here, but also the number of site mean directions used in each of the paleomagnetic data sets to calculate the mean poles (Table 2, Fig. 2). We suggest that the variability in the pole positions is a direct consequence of the small size of the individual sample sets, the inclusion of data that duplicate other spot readings, and the inclusion of spot readings that are not statistically equivalent (e.g., high versus low Fisher precision parameters), such that most of these individual studies do not provide a robust characterization of the time-averaged geomagnetic field. The dispersion (S) of VGPs calculated from the site mean directions for most of the individual studies is either greater or smaller than can be straightforwardly explained by the secular variation of the geomagnetic field (e.g., Johnson et al., 2008) and the A95 values plot outside of the Deenen envelope (Deenen et al., 2011). These observations challenge the interpretation that these individual poles can be used for paleogeographic reconstructions.

We also note that Liebke et al. (2012) suggested that the mixed polarity observed in many of the dikes presented in Liebke et al. (2010) is primary and is the product of multiple injection episodes within each dike, such that each dike partially averages paleosecular variation. While we acknowledge this possibility, there is no reported independent field evidence for multiple injection episodes within the narrow (1–3 m) dikes. For simplicity, and in an effort to apply our selection criteria uniformly to all data sets, we will assume that each dike represents a single injection episode that can be treated equivalently to a lava unit. Notably, the exclusion of site mean directions from Liebke et al. (2010) from our final analysis does not significantly change the position of the mean paleomagnetic pole calculated for the Linzizong Formation and therefore does not change the paleolatitude of the southern margin of Asia ca. 50 Ma (see following).

We test the robustness of these individual paleomagnetic poles by combining site-mean directions from all of these studies and calculating a mean paleomagnetic pole from the VGP distribution (Fig. 2). If each individual study represents secular variation, then in principle, these individual poles should statistically overlap with the mean Linzizong Formation paleomagnetic pole. The data quality filter (described in Methods discussion) excludes 21 of 62 reported lava site mean directions (selecting from only sites used by the original authors of each study; Table A1 (see footnote 1). The mean paleomagnetic pole in tilt-corrected coordinates is located at $\lambda = 80.2°N$, $\phi = 230.4°E$ ($K = 30.5$, A95 = 4.1° (A95$_{min}$ = 3.9°; A95$_{max}$ = 7.9°), S = 14.8°, n = 41) (Tables 1 and 2). The 41 site mean directions used to calculate this filtered paleomagnetic pole include data from each of the five independent studies and pass a regional fold test at 95% confidence (χ^2 test of McFadden, 1990). Although these data do not pass a reversal test at 95% confidence (class C: $\gamma_{calculated} = 15.8°$, $\gamma_{critical} = 11.5°$; McFadden and McElhinny, 1990), we note that
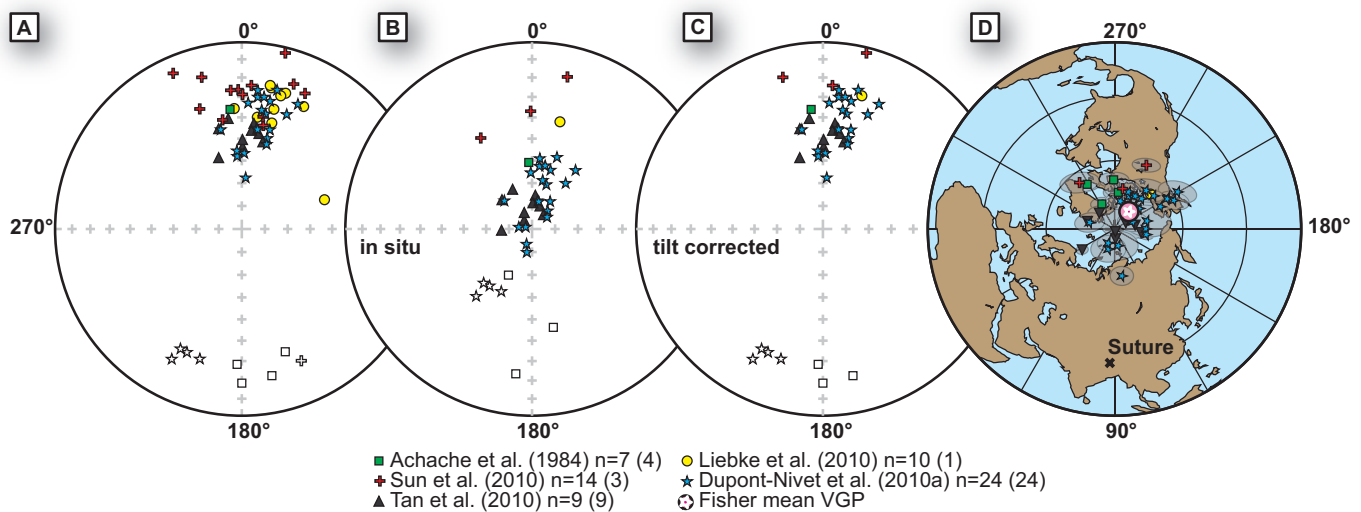
Figure 2. Paleomagnetic data from the Linzizong Formation (LZF). Closed symbols indicate normal polarity directions; open symbols indicate reversed polarity directions. VGP—virtual geomagnetic pole. (A) Site mean directions from the LZF before the population has been filtered for consistent statistical quality (used by original authors of each study, N = 62). (B) Site mean directions from the LZF after the population has been filtered for consistent statistical quality (N = 41); in situ coordinates. (C) Same as B, except in tilt-corrected coordinates. (D) Paleomagnetic pole for the LZF calculated from the virtual geomagnetic poles (VGPs) of the paleomagnetic data shown in C. In the legend, *n* refers to the number of spot readings provided by each study; number in parentheses is number of spot readings that meet our quality criteria.

the reversal test may not be ideally suited for sequences of extrusive rocks because individual eruptive events and even subsets of eruptive events (e.g., lavas that erupted during a single reversed or normal polarity interval) may not provide a time-averaged representation of the geomagnetic field (i.e., average paleosecular variation). The fact that a normal-reverse-normal polarity sequence is recorded within a long interval of lavas, however, is strong evidence that the lavas record primary directions and record several hundreds of thousands to millions of years of time. It is important that the calculated dispersion of this filtered mean VGP is consistent with known dispersion caused by paleosecular variation (Johnson et al., 2008), the A95 is within the confidence envelope of Deenen et al. (2011), and the pole fulfills all

seven quality criteria of van der Voo (1990). We conclude that this paleopole more accurately characterizes the time-averaged behavior of the geomagnetic field than any previous individual study of the Linzizong Formation.

Notably, only in Dupont-Nivet et al. (2010a) were paleomagnetic data assessed for direction grouping. Ideally, we would like to assess all of the Linzizong Formation site mean directions for appropriate direction grouping to ensure that only independent samples of the geomagnetic field direction are averaged, but we are currently limited by the stratigraphic fingerprinting of regionally extensive lavas in the Linzizong Formation. For example, Tan et al. (2010) presented nine site mean directions over a short interval in outcrop, but only six of these directions are

TABLE 2. PALEOMAGNETIC POLES FOR THE PANA MEMBER (UNIT T2) OF THE LINZIZONG FORMATION

Study	Filtered	N	Pole latitude (°N)	Pole longitude (°E)	A95	K	S	A95$_{min}$	A95$_{max}$	I$_p$	±	ΔI$_p$
Achache et al. (1984)	no	7	72.7	287.6	8.8	47.7	11.8	7.8	24.1	12.6	±	8.8
	yes	4	72.5	283.4	8.6	114.6	7.6	9.8	34.2	12.1	±	8.6
Tan et al. (2010)	no	9	89.6	271.6	6.6	62.0	10.3	7.1	20.5	28.6	±	6.6
	yes	9	89.6	271.6	6.6	62.0	10.3	7.1	20.5	28.6	±	6.6
Dupont-Nivet et al. (2010a)	no	31	76.7	208.6	4.7	31.3	14.5	4.3	9.4	21.7	±	4.7
	yes	24	77.6	211.6	5.0	35.7	13.6	4.8	11.1	21.7	±	5.0
Liebke et al. (2010)	no	10	70.2	210.6	12.9	17.0	20.1	6.8	19.2	17.2	±	12.9
	yes	1	68.1	224.2	–	–	–	–	–	12.4	±	–
Sun et al. (2010)	no	14	74.0	274.4	8.4	23.1	16.9	5.9	15.6	13.1	±	8.4
	yes	3	67.7	268.2	23.9	27.6	15.5	11.0	41.0	6.7	±	23.9
Mean pole (this study)	no	62	79.1	236.8	3.8	23.1	17.1	3.3	6.1	19.5	±	3.8
	yes	41	80.2	230.4	4.1	30.5	14.8	3.8	7.9	21.1	±	4.1
	yes*	17	80.9	269.5	6.4	32.3	14.3	5.5	13.8	19.9	±	6.4

Note: Conventions and symbols as in Table 1. Filtered: mean virtual geomagnetic pole (VGP) calculated without or with applying the data quality filter described in the text (yes*—filtered pole without the results of Dupont-Nivet et al., 2010a). Dashes (blanks) in Liebke et al. (2010) column are because this pole results from only one VGP.

stratigraphically independent (following Mankinen et al., 1985). Moreover, the results from Tan et al. (2010) overlap with a few of the stratigraphically highest sites reported in Dupont-Nivet et al. (2010a). Thus, our new pole, which incorporates all statistically robust site mean data from paleomagnetic studies of the Linzizong Formation, almost certainly contains some non-independent data, but we maintain that this remains the most comprehensive and statistically consistent pole for the Linzizong Formation. The corresponding 56–47 Ma paleolatitude of the reference site on the IYSZ is 21° ± 4°N.

Inspection of Figure 2 and Tables 2 and A1 (see footnote 1) suggests that the filtered data set favors our own results (Dupont-Nivet et al., 2010a). We note that this is the result of the large size of the Dupont-Nivet et al. (2010a) data set and that the same quality control in the original study was applied in this study, so no direction groups were culled from the compilation. To test if the large data set of Dupont-Nivet et al. (2010a) biases the mean Linzizong Formation paleopole, we recalculated the pole using only the filtered data described here and excluding the site mean directions from Dupont-Nivet et al. (2010a). The resulting pole is calculated from 17 tilt-corrected site mean directions and is located at $\lambda = 80.9°N$, $\phi = 269.5°E$ (K = 32.3, A95= 6.4°; $A95_{min} = 5.5°$; $A95_{max} = 13.8°$, S = 14.3°). A simple F-test indicates that the filtered Linzizong Formation poles with and without the Dupont-Nivet et al. (2010a) data are not significantly different at high confidence levels (p = 11.48%). We conclude that the large data set of Dupont-Nivet et al. (2010a) does not significantly bias the mean Linzizong Formation pole.

In summary, we have combined site mean directions provided by six independent paleomagnetic studies of the Linzizong Formation to calculate a new paleomagnetic pole for the Lhasa terrane in early Eocene time. After filtering the original 62 site mean directions to produce a data set composed of statistically consistent site mean directions, we calculated a mean pole located at $\lambda = 80.2°N$, $\phi = 230.4°E$ (K = 30.5, A95= 4.1°, S = 14.8°) (Fig. 2). The 41 underlying site mean directions used to calculate this pole pass a paleomagnetic fold field test at high confidence, exhibit a reversal stratigraphy, are characterized by a VGP dispersion that is in excellent agreement to that observed in 0–5 Ma lavas sampled at the same latitude at Lhasa, and exhibit scatter in the data set that can be straightforwardly explained by paleosecular variation. We conclude that this pole is the most statistically comprehensive and coherent paleomagnetic pole from Tibetan Asia for the Cenozoic and is ideally suited to provide (1) the paleolatitude of the Tibetan Plateau, (2) precise paleomagnetic constraints on the age and latitude of the collision between the Tibetan Himalaya and the Lhasa terrane, and (3) the distribution of convergence within the India-Asia collisional orogen.

Late Cretaceous Redbeds, Maxiang

Sun et al. (2012) reported paleomagnetic data from the 86 ± 14 Ma Shexing Formation of redbeds that crop out along the Lhasa-Golmud highway near Maxiang (Fig. 1). Site mean direc-

tions calculated from the high-temperature ChRM component pass a fold test at high confidence. We evaluated the distribution of high-temperature specimen directions for inclination shallowing following the elongation/inclination (E/I) method of Tauxe and Kent (2004) (original ChRM directions provided by Zhiming Sun, 2011, personal commun.). Samples with mean angular deviations of ChRM directions >15° (n = 5) and with reversed polarity ChRM (n = 2) directions were removed from the population to exclude poorly resolved or transitional directions. The Vandamme cut-off procedure for identifying outliers in the direction population (Vandamme, 1994) removed another seven samples, resulting in a mean VGP for the Shexing Formation located at $\lambda = 70.5°N$, $\phi = 324.9°E$ (samples corrected = 100, K = 32.5, A95 = 2.5°; $A95_{min} = 2.7°$; $A95_{max} = 4.5°$, S = 14.3°). We calculated a flattening factor of 0.66 (0.53 and 0.91 95% confidence interval; Fig. 3), resulting in an E/I corrected mean VGP located at $\lambda = 74.6°N$, $\phi = 346.5°E$ (N = 100, K = 28.6, A95= 2.7°; $A95_{min} = 2.7°$; $A95_{max} = 4.5°$, S = 14.3°). These results suggest ~9° of inclination shallowing in the fluvial-lacustrine redbeds of the Shexing Formation, which is typical of these facies in Asia (Dupont-Nivet et al., 2010b; Lippert et al., 2011). The calculated A95 is at the lower limit of the minimum value predicted by geomagnetic field models; i.e., paleosecular variation is at the threshold of being represented by this data set. This can be straightforwardly explained by some averaging of secular variation within individual specimens, which is common in sediments and especially redbeds (Deenen et al., 2011). The calculated paleolatitude for the reference location on the IYSZ is 24.9 ± 2.7°N at 86 ± 14 Ma.

Late Cretaceous Redbeds, Penbo

We use paleomagnetic data from the nonmarine Takena Formation and calculations of a Late Cretaceous (97 ± 7 Ma; Leier et al., 2007a) paleolatitude for the Lhasa block of Tan et al. (2010). The distribution of the sample directions from this data set is consistent with inclination shallowing that is readily attributed to sedimentary depositional processes. Tan et al. (2010) corrected these directions using the E/I method. The paleomagnetic pole calculated from these tilt and inclination shallowing corrected sediments is located at 79.6°N, 329.9°E (N = 377, A95= 2.2; $A95_{min} = 1.6°$; $A95_{max} = 2.0°$) (Table 1). The calculated A95 is slightly higher than expected from paleosecular variation alone, suggesting some additional error due to local rotations between sampling localities, bedding measurement errors, the inclusion of outlier directions, or a combination of these factors. Taking these data at face value, the paleolatitude of the reference location on the IYSZ calculated from this pole is 23.7° ± 2.2°N ca. 97 ± 7 Ma.

Tan et al. (2010) reported paleomagnetic data from what they described as 32 consecutive, 2–30-cm-thick lavas interbedded with the Takena Formation. We do not use these data because 2–30 cm is unusually thin for lavas and no pictures or further descriptions of these rocks were provided, and because our own field observations, as well as the comprehensive field study of
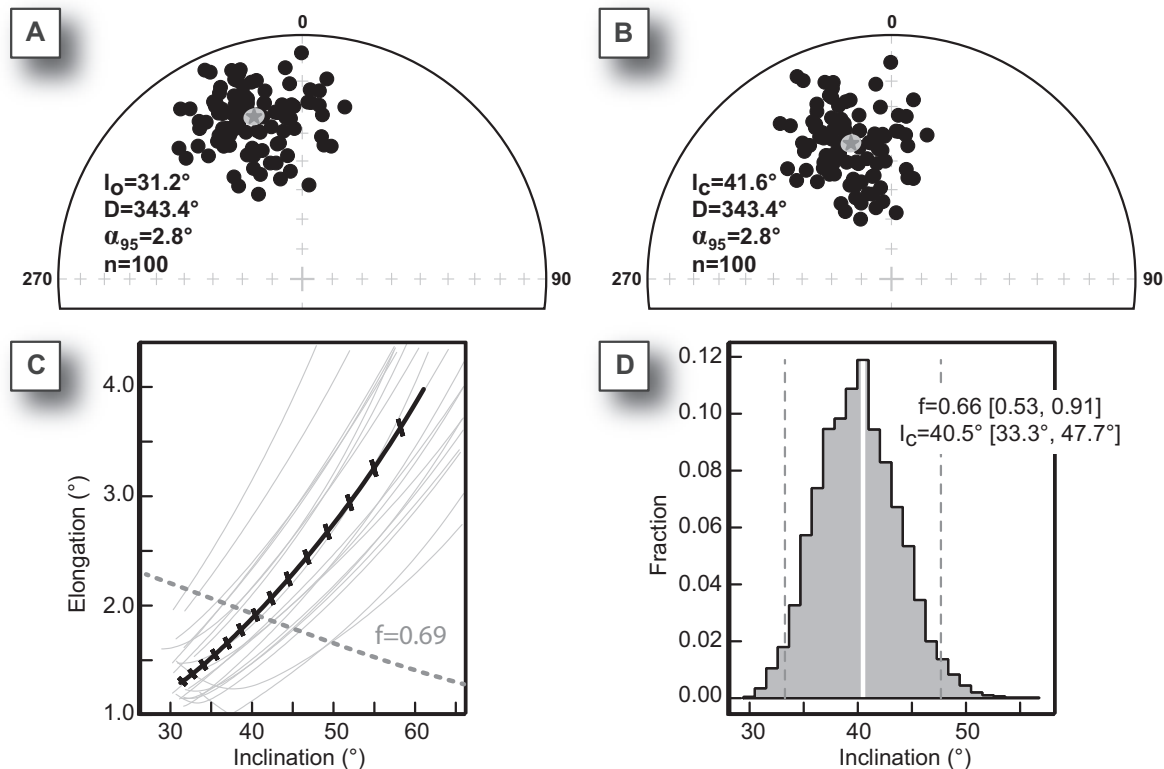
Figure 3. Elongation/inclination (E/I) correction (Tauxe and Kent, 2004) of high-temperature, primary magnetization component of the Shexing Formation redbeds at Maxiang, south-central Lhasa terrane (Sun et al., 2012). D—declination; n—number of samples; α_{95}—half angle of the 95% confidence cone on the mean direction. (A) Equal area plot of original paleomagnetic directions in tilt-corrected coordinates, with a mean inclination (I_o) of 31.2° (gray star, 95% confidence interval indicated in surrounding light gray). Slight horizontal elongation of the direction distribution is consistent with sedimentary inclination shallowing. (B) E/I-corrected paleomagnetic directions after accounting for a flattening factor of 0.66. The E/I-corrected inclination (I_c) is 41.6°. (C) Plot of elongation versus inclination for the TK03.GAD (Tauxe and Kent, 2004) paleosecular variation model (bold dashed gray line) and for the Shexing Formation directions (bold barbed black line) for different flattening factors, f. Thin light gray lines are the results from 20 boot-strapped data sets. The crossing points of the Shexing Formation and bootstrapped data set with the TK03.GAD results represents the elongation/inclination pairs that are most consistent with the TK03.GAD field model. (D) Histogram of crossing points from 5000 boot-strapped data sets. The most frequent flattening factor is f = 0.66, resulting in the distribution of directions shown in B.

Leier et al. (2007a), did not identify any lavas within the Takena Formation. There are, however, widespread sills and dikes (e.g., He et al., 2007; Liebke et al., 2010) commonly with early Eocene $^{40}Ar/^{39}Ar$ whole-rock (Yue and Ding, 2006) and U/Pb zircon ages (He et al., 2007).

We also note that we have not used paleomagnetic data from the Takena Formation reported by Lin and Watts (1988). The reasons for this are (1) Lin and Watts (1988) provided only site mean directions from their sampling sites, whereas individual sample ChRM directions are needed to evaluate these results for sedimentary inclination shallowing. (2) Tan et al. (2010) resampled some of the same horizons as Lin and Watts (1988). Inclusion of these results would lead to oversampling of the geomagnetic field, resulting in spurious or misleading sampling statistics. It is neither necessary nor justified to include the Takena paleomagnetic from Lin and Watts (1988) in our compilation.

Early Cretaceous Lavas

Paleomagnetic results from volcanic rocks of Cretaceous age have been reported in two recent studies. Sun et al. (2012) reported 15 site mean directions from the 114.2 ± 1.1 Ma Worong-gou Formation rhyolites near Deqing, on the west shore of Nam Co (Fig. 1; Table A2 [see footnote 1]); only five site mean directions meet our data quality standards. Chen et al. (2012) reported 19 site mean directions from 120 ± 10 Ma tuffs and lavas of the Zenong Group near the town of Cuoqin in the central Lhasa terrane (Fig. 1; Table A2 [see footnote 1]); only nine site mean directions describe the geomagnetic field at this locality after the data are filtered for consistent quality.

We combine the filtered results of these two studies to calculate a lava-based paleomagnetic pole from the Early Cretaceous of the Lhasa terrane. Although both localities show

similar inclinations, the declinations vary by ~30°–40°, implying significant rotations between the two sampling regions (Fig. 4). We follow Doubrovine and Tarduno (2008) and calculate a maximum likelihood virtual geomagnetic latitude (VGL) using the Arason and Levi (2010) method. First, we calculate the VGPs for the filtered site mean directions and then calculate the VGL of the reference site on the IYSZ. These VGLs are then used as input to calculate the maximum likelihood latitude for the reference site from these data: 16.2° ± 3.6°N at 120 ± 10 Ma. We note, however, that the dispersion of these VGLs is only 7.0°, suggesting that paleosecular variation has been underrepresented by the lavas. We caution that this paleolatitude estimate maybe not be robust.

IMPLICATIONS: DISCUSSION

Latitude of the Southern Lhasa Terrane since the Early Cretaceous

The paleomagnetic data described above record the latitude of the southern margin of the Lhasa terrane since ca. 110 Ma (Fig. 5). These latitudes are calculated from paleomagnetic data from well-dated lavas and sediments that mostly appear to average short-term geomagnetic field behavior (i.e., secular variation) and have been corrected for sedimentary inclination shallowing biases. We emphasize that the paleolatitude curve shown in Figure 5 is calculated from the statistically most comprehensive

and consistent paleomagnetic data set currently available for the Lhasa terrane from 85° to 91°E.

Figure 5 shows that the Lhasa terrane has remained relatively stable in terms of latitude since the Early Cretaceous. Notably, none of the paleomagnetic data sets is consistent with low, tropical latitudes for the Lhasa terrane, in contrast to conclusions drawn from some individual studies based on small data sets associated with high dispersion (Westphal et al., 1983; Lin and Watts, 1988; Chen et al., 2010). Instead, the Lhasa terrane was positioned at high tropical to low subtropical north latitudes (16°–22°N) since ca. 110 Ma and has translated northward to its present latitude at 29°N only in the past 50 m.y. Part of this motion can be attributed to the absolute plate motion of Eurasia relative to the spin axis described in the GAPWP (Torsvik et al., 2012), and part is related to north-south shortening of the Asian plate, e.g., in the Tibetan Plateau and the Tien Shan (e.g., Molnar and Tapponnier, 1975; Dewey et al., 1989; van Hinsbergen et al., 2011a). This latitude history is a key boundary condition for interpreting the kinematics and geodynamics of the India-Asia convergence history and tectonics and climate of the Lhasa terrane and surrounding region. Each of these topics is discussed in the following.

Paleomagnetic Estimate of the Age of the Tibetan Himalaya–Lhasa Collision

The onset of continental collision between India and Asia is of paramount interest to many Earth scientists because it is conventionally thought to mark the onset of surface uplift of the
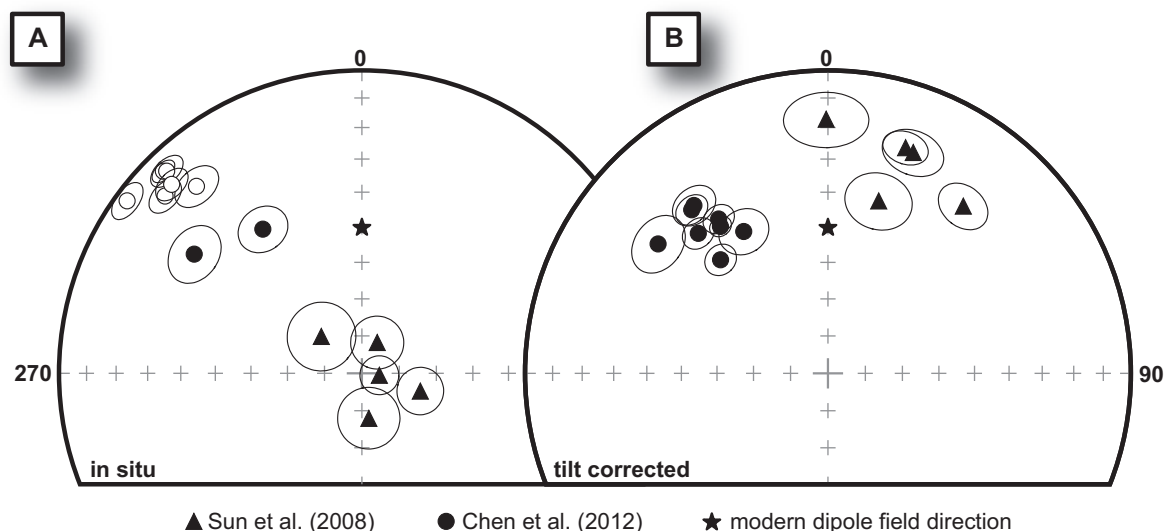

Figure 4. Equal area plot of site mean directions from Early Cretaceous volcanic rocks from the central and western Lhasa terrane that pass our data quality criteria (Sun et al., 2008; Chen et al., 2012). (A) In situ coordinates. (B) Tilt-corrected coordinates. Downward pointing directions are shown as filled symbols; upward pointing directions are shown as open symbols. Significant improvement in the clustering of inclinations from in situ coordinates to tilt-corrected coordinates is consistent with a prefolding magnetization. The noticeably different declination values observed in the two localities are consistent with differential vertical axis rotation since the emplacement of these lavas and justify the use of latitude-only data analysis methods (see text for details).

Tibetan Plateau (but see following discussion), and because it is the archetypal setting for many models about the dynamics of continental subduction (e.g., Chemenda et al., 2000; Capitanio et al., 2010). Moreover, the demise of the Neotethyan Ocean should impart significant changes in plate force balances and ocean circulation. The age of the onset of collision between continental units of India and Asia is a key boundary condition for understanding the geodynamics governing the distribution of strain in subduction zones and collisional orogens, because, with the use of the plate circuits (e.g., Molnar and Stock, 2009; Copley et al., 2010; van Hinsbergen et al., 2011b), it sets the budget for the magnitude of plate convergence that must be accounted for within the orogen. It is this last point that makes knowing the India-Asia collision age especially important.

The end of marine sedimentation within the Tibetan Himalaya (Rowley, 1996; Garzanti, 1999; Green et al., 2008; Najman et al., 2010; Hu et al., 2012) in the early Eocene and the appearance of Asian detritus in Tibetan Himalaya sediments by 52 Ma (Najman et al., 2010; Wang et al., 2011; Hu et al., 2012) are generally considered to reflect the accretion of the Tibetan Himalaya to the Asian plate at that time (see review by Najman et al., 2010). This time period also corresponds to a nearly two-fold decrease in the relative motion rates between the Indian and Asian plates, which has been interpreted to represent the arrival of buoyant, extended continental margin crust to the subduction zone beneath southern Tibet, as well as increased resistance at the subduction zone due to surface uplift above the trench (Iaffaldano and Bunge, 2009; van Hinsbergen et al., 2011b).

Paleomagnetism can be used to independently estimate the Tibetan Himalaya–Asian collision age by determining when paleolatitudes of the Tibetan Himalaya and southern Tibet start to overlap. Previous paleomagnetic-based arguments have produced Tibetan Himalaya–Asia collision ages that range from 70 Ma (Klootwijk et al., 1992) to ca. 35 Ma (Ali and Aitchison, 2006) and several ages between (e.g., see individual Linzizong Formation studies noted above). The disparity of collision ages results from (1) the use of data from sedimentary rocks that have not been evaluated for sedimentary inclination shallowing; (2) the use of data from lavas that insufficiently represent secular variation; or (3) using APWPs of the stable continents, or only selected data from India and Eurasia while disregarding plate circuits altogether and inferring dimensions of Greater India and greater Asia without taking paleomagnetic evidence into account (e.g., Ali and Aitchison, 2006).

The paleolatitude history of the Lhasa terrane described here and a recent reappraisal of high-quality paleomagnetic data of primary origin from Late Cretaceous to late Paleocene marine sediments from the southern Tibetan Himalaya (Patzelt et al., 1996; Yi et al., 2011; see also van Hinsbergen et al., 2012b) can be used to estimate a paleomagnetic collision age. Using a reference point located at 29°N, 88°E on the IYSZ, the latitude of the northern Tibetan Himalaya overlaps with the latitude of the southern margin of the Lhasa terrane at 49.4 ± 4.5 Ma, at lat 21° ± 4°N (95% confidence intervals; see Fig. 5A). This age is

Figure 5 (*on following page*). The age and latitude of the Tibetan Himalaya–southern Tibet collision as calculated from paleomagnetic data discussed in the text and presented in Table 1. Paleolatitude versus time is shown for a point on the modern Indus-Yarlung suture zone (29°N, 88°E) in Eurasia (gray), southern Lhasa terrane, Tibetan Himalayan, and India reference frames. APWP—apparent polar wander path. (A) Without accounting for crustal shortening within the Indus-Yarlung suture zone (IYSZ) during and since collision, paleomagnetic data indicate that the collision between the Tibetan Himalaya and southern Tibet occurred ca. 49.5 ± 4.5 Ma at 21° ± 4°N (95% confidence interval). (B) With conservative estimates of the magnitude of crustal shortening (see text for details), the paleomagnetically determined collision age is ca. 52.5 ± 4.5 Ma at 19° ± 4°N (95% confidence interval).

entirely consistent with estimates derived from geologic observations for the collision described.

We emphasize that this paleomagnetically determined collision age is a minimum estimate. The paleolatitudes calculated here describe the location of the suture that currently separates the Tibetan Himalaya from Asian crustal units. It is likely, however, that prior to collision, the Neotethyan subduction zone was separated from Asia by a forearc. At present, the southern Lhasa terrane immediately adjacent to the suture hosts the Gangdese volcanic arc (of which the Linzizong Formation is part), which formed since Early Cretaceous time during northward subduction of the Neotethyan Ocean (Ji et al., 2009). Prior to collision, however, a forearc must have separated the Gangdese arc from the subduction zone; relics of a Cretaceous forearc are preserved in the IYSZ (Einsele et al., 1994; Yin et al., 1994). There are no direct constraints on the original width of this forearc, but typical arc-trench distances today are ~200–300 km wide (modern observations using GeoMapApp; http://www.geomapapp.org). The initial collision between the Tibetan Himalaya and southern Tibet may have occurred ~2° south of the modern southern boundary of the Lhasa terrane (i.e., the suture). After accounting for the shortened Gangdese forearc, we predict that the southern margin of Asia may have been located at 19° ± 4°N ca. 50 Ma.

In addition, the collision age is calculated based on the modern northernmost exposures of Paleocene rocks of the Tibetan Himalaya. If Tibetan Himalayan rocks existed farther north, but were underthrusted entirely below the Lhasa terrane, initial collision could have been older. For example, crustal shortening of the Tibetan Himalayan sequence north of Duela and Gamba, where the Tibetan Himalaya paleomagnetic data were collected, is unconstrained by detailed field studies; it may be as much as 50% or more (Ratschbacher et al., 1994; Ding et al., 2005), accounting for another ~1° of more northern latitude for the leading edge of the Tibetan Himalaya terrane prior to collision.

We conservatively add 2° of latitude to the leading edge of both the Tibetan Himalaya and southern Tibet to estimate the effect of postcollisional shortening within the IYSZ on the paleomagnetic collision age. Given the very high plate convergence rates between 60 and 50 Ma (16–18 cm/yr; van Hinsbergen et al., 2011b), these modifications would have only a minor effect on

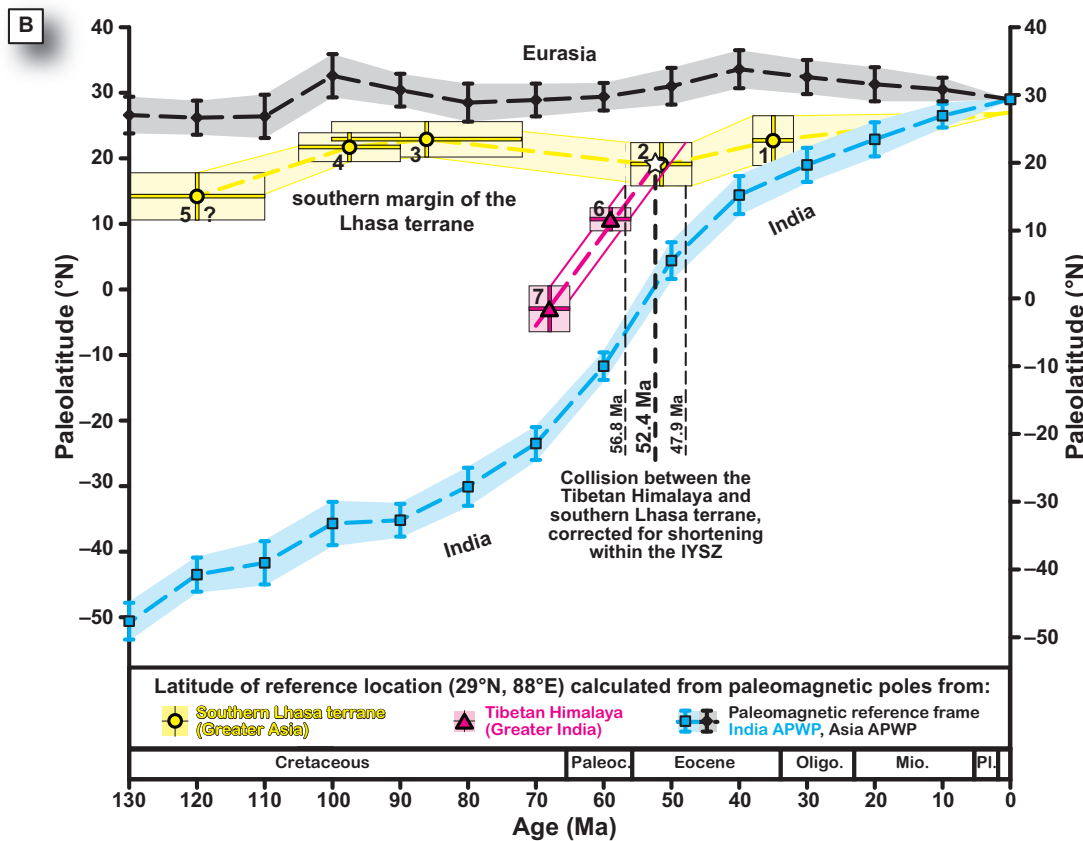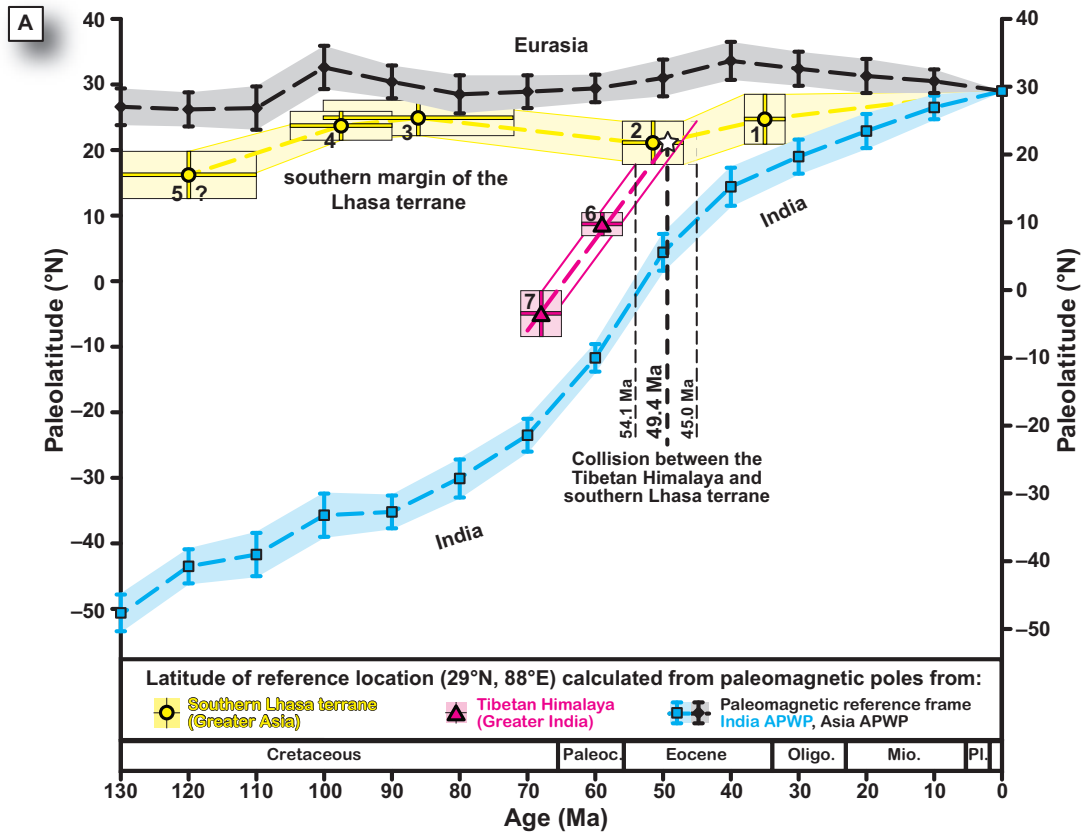*Early Cretaceous–present latitude of the proto-Tibetan Plateau*

Figure 5.

the collision age, which would be pushed back to 52.4 ± 4.5 Ma at 19° ± 4°N (95% confidence). We emphasize that although these shortening corrections appear reasonable, the actual magnitude of shortening within the Xigaze forearc, IYSZ, and Tibetan Himalaya fold-thrust belt remains poorly determined by geologic studies. Nevertheless, the mean IYSZ shortening-corrected collision age is in even better agreement with the stratigraphic record of collision, which indicates that the Tibetan Himalaya was close enough to Asia by 52 Ma to be a sink for Asian-derived detritus (e.g., Najman et al., 2010; Wang et al., 2011; Hu et al., 2012). The preponderance of geological and geophysical data from the IYSZ indicates that collision between continental units of Indian affinity with the southern margin of Asia was ongoing by 52 Ma. Until improved estimates of crustal shortening within the suture zone become available, we take a conservative approach and conclude that this collision occurred at ~21° ± 4°N.

Distribution of Strain in the India-Asia Collisional Orogen

Collision at 52 Ma implies that ~2860–3600 km of India-Asia plate convergence (from the western to eastern syntaxes) must be accounted for in the Himalaya-Tibetan orogen (van Hinsbergen et al., 2011b, 2012b). However, the plate circuit from which these convergence budgets are calculated cannot predict where this convergence is distributed, and therefore how and where strain accumulates in the India-Asia collisional orogen. The paleolatitude record for the Lhasa terrane described herein provides a fundamental, first-order constraint on this problem by locating the southern margin of Asia within the India-Asia plate circuit. Comparing the ca. 52 Ma collision of lat ~21° ± 4°N calculated for the IYSZ in southern Tibet coordinates to the 31° ± 3°N paleolatitude predicted from the GAPWP in Eurasian coordinates (Torsvik et al., 2012) suggests that ~1100 ± 560 km of convergence was consumed between southern Tibet and stable Asia. This magnitude of convergence is larger than the amount of shortening (600–1500 km from eastern Tibet to the Pamir) north of the IYSZ since 50 Ma, calculated from structural geologic estimates (van Hinsbergen et al., 2011a). However, it has long been recognized that paleomagnetic inclinations across Central and East Asia (e.g., in Mongolia, north of the region that accommodated the majority of Cenozoic shortening related to India-Asia convergence; Hankard et al., 2007; Dupont-Nivet et al., 2010b) are also significantly shallower in Cenozoic time than predicted by the GAPWP. Therefore, the calculated paleolatitude difference computed from the paleolatitude of the Lhasa terrane compiled here, and that predicted by the GAPWP (Torsvik et al., 2012), cannot entirely be ascribed to India-Asia collision-related shortening of Tibet. Previous proposals to explain the Asian inclination shallowing include (1) non-dipole contributions (Si and Van der Voo, 2001), (2) mobility of Asia relative to Eurasia along cryptic faults in the Urals and along the Tornqvist-Tesseyre line (Cogné et al., 1999, 2013; Hankard et al., 2007), or (3) a combination of time-dependent non-dipole contributions and imperfections in the GAPWP (Dupont-Nivet et al., 2010b). For a

detailed discussion of the Asian inclination shallowing problem, including possible solutions and important implications, there are reviews (Dupont-Nivet et al., 2010b; Lippert et al., 2011). What is clear from the paleomagnetic and structural studies (Dewey et al., 1989; Searle et al., 2011; van Hinsbergen et al., 2011a) of the Tibetan orogen is that the magnitude of convergence and upper crustal shortening within Asia since ca. 50 Ma is on the order of hundreds, not thousands of kilometers, as once assumed based on pioneering paleomagnetic and structural studies (e.g., Achache et al., 1984; Lin and Watts, 1988; Tapponnier et al., 1982).

A direct, but often overlooked, implication from nearly all studies of the Tibetan orogen is that all convergence since 50 Ma that was not accommodated north of the IYSZ by intra-Asian deformation must consequently have been accommodated south of the IYSZ by Indian plate subduction. The paleomagnetic data from the Lhasa terrane reviewed herein, and those data compiled from the Tibetan Himalaya (Patzelt et al., 1996; Yi et al., 2011; see also van Hinsbergen et al., 2012b) show that as much as ~2440 ± 330 km of convergence was accommodated between the Tibetan Himalaya and Himalayan front. This amount of convergence far exceeds the minimum shortening estimates for the Greater and Lesser Himalayan thrust belts (400–700 km; DeCelles et al., 2002; Long et al., 2011), and those of the few structural studies of the Tibetan Himalaya (100–200 km; Ratschbacher et al., 1994; Wiesmayr and Grasemann, 2002; Murphy and Yin, 2003). It follows from the paleomagnetic reconstructions that a large part of Greater India lithosphere has no as-yet recognized record at the surface (due largely to a combination of erosion and underthrusting). Paleomagnetic and plate kinematic data clearly indicate that in Late Cretaceous time Greater India was considerably more extensive (as much as 3000 km beyond modern cratonic India) than in the Early Cretaceous and before (<900 km) (van Hinsbergen et al., 2012b). Van Hinsbergen et al. (2012b) argued that Cretaceous Greater India consisted of thinned continental and oceanic lithosphere (Greater India Basin) resulting from a ca. 120–70 Ma rifting event that separated a microcontinent carrying the Tibetan Himalayan rocks from the Indian craton. Others have previously suggested extension within Greater India, although the timing and the implications for the India-Asia collision are different (Roy, 1976; Appel and Li, 1988; Hsu et al., 1995; Patzelt et al., 1996). Van Hinsbergen et al. (2012b) concluded that the ca. 52 Ma Tibetan Himalaya–Asia collision was characterized by a microcontinent-continent collision (Fig. 6), followed by subduction of the Cretaceous Greater India Basin beneath the southern margin of Asia, and then by collision between cratonic India and Asia at 25–20 Ma.

Surface Uplift of the Tibetan Plateau, Paleogeography of the India-Asia Collision Zone, and Implications for Atmospheric Dynamics and Regional Climate

The onset of surface uplift of the Tibetan Plateau from near sea level is generally considered to have begun shortly after the onset of collision between the Tibetan Himalaya and southern

Figure 6. Early Eocene paleogeographic reconstruction of the Neotethyan region at the time of collision between the Tibetan Himalayan micro-continent and the southern margin of Asia. Key distinctions between this reconstruction and previous reconstructions include the elevated Lhasa-plano (Kapp et al., 2005) (i.e., proto–Tibetan Plateau) and the oceanic Greater India Basin (van Hinsbergen et al., 2012b). Neotethyan subduction zone (bold red line) reconstruction is after van Hinsbergen and Schmid (2012), van Hinsbergen et al. (2012b, 2014), Gaina et al. (2013), Agard et al. (2011), Argnani (2012), and Hall (2012). Paratethys region (e.g., Turan Sea, Tarim Basin) reconstruction is after Bosboom et al. (2011, and references therein).

Tibet, such that the Tibetan Plateau is often considered to be the result (almost) entirely of the India-Asia collision (Molnar and Tapponnier, 1975; England and Houseman, 1986; Tapponnier et al., 2001; Royden et al., 2008; Clark, 2012). However, several lines of geologic evidence challenge this simplified view of the surface uplift history of the Tibetan Plateau. Northward sub-duction of the Neotethys Ocean below the Lhasa terrane began shortly after the collision of the Lhasa terrane with the Qiang-tang terrane to the north in latest Jurassic–earliest Cretaceous time (Maluski et al., 1982; Leier et al., 2007b; Zhu et al., 2009). Also in Cretaceous time, and so well before the Tibetan Hima-laya–Lhasa collision, well-documented fold and thrust fault belts developed on the Lhasa terrane (~250 km of north-south shorten-ing) and Qiangtang terrane (~400 km of north-south shortening) (Kapp et al., 2005, 2007a, 2007b; Leier et al., 2007a; Volkmer et al., 2007; Pullen et al., 2008). Marine sedimentation through-out the northern Lhasa and southern Qiangtang terranes ceased during Aptian time (Zhang, 2000; Kapp et al., 2007a; Leier et al., 2007a), even though this period of time corresponds to global sea-level highstands (Müller et al., 2008), indicating that crustal thickening had been sufficient to raise the surface elevation of Tibet above sea level since ca. 110 Ma. Thus, a proto–Tibetan Plateau probably developed in Cretaceous-Paleogene time and characterized the physiography of the southern margin of Asia from at least 45 Ma (Dupont-Nivet et al., 2008; Wang et al., 2008; Rohrmann et al., 2012), and probably even Late Cretaceous time

(England and Searle, 1986; Murphy et al., 1997; Kapp et al., 2005, 2007a, 2007b; Searle et al., 2011). The stable oxygen isotope paleoaltimetry record from Tibet, albeit limited and reliant on numerous assumptions, is generally consistent with an Eocene proto-plateau (see recent review by Quade et al., 2011). Therefore, a significant part of the shortening within (van Hinsbergen et al., 2011a, and references therein) and surface uplift (see references in preceding two sentences) of the Tibetan Plateau predate the Tibetan Himalaya–Lhasa collision. We note that an important implication of the two-stage India-Asia collision as proposed by van Hinsbergen et al. (2012b) is that almost all surface uplift and shortening of Tibetan lithosphere, except for northeastern and possibly eastern Tibet (e.g., Kirby et al., 2002; Dettman et al., 2003; Hough et al., 2011; Zhuang et al., 2011; Lease et al., 2012) probably predate the final continent-continent collision (ca. 25–20 Ma). Numerous geologic studies indicate that crustal shortening and surface uplift in northeastern and eastern Tibet were also substantial before this time (Jolivet et al., 2001; Horton et al., 2002, 2004; Richardson et al., 2008; Yan et al., 2011; Zhuang et al., 2011; Wang et al., 2012). Although the shortening and surface uplift of the Tibetan Plateau is usually ascribed to the collision between India and Asia, the evidence and arguments listed here instead suggest that the Tibetan Plateau may be quite similar to the Altiplano of the Andes, in that most crustal shortening and plateau uplift developed above an oceanic subduction zone in the absence of a continent-continent collision. Also similar to the Andes, most of the proto- and modern Tibetan Plateau developed at dry, subtropical latitudes.

Another important implication of the paleolatitude of the Lhasa-plano (i.e., proto–Tibetan Plateau) during the two-stage India-Asia collision history described in van Hinsbergen et al. (2012b) is that throughout the Paleogene a deep tropical to subtropical oceanic basin remained between the high topography of the proto-Himalaya and Lhasa-plano to the north and continental India to the south. This Greater India Basin (van Hinsbergen et al., 2012b) would have connected the Indonesian seaways to the eastern Mediterranean Tethys (Fig. 6). Thus, east-west oceanic and atmospheric circulation in the Tethys may have been sustained much longer than normally assumed, although the details of through-going circulation depend on the latitude and depth of the seaway. Both circulation at tropical to subtropical latitudes and the presence of a deep and large body of water undoubtedly had a prolonged and profound effect on the paleoclimate in the region, particularly in terms of the Indian monsoon, physical and chemical weathering, and carbon burial.

For example, the modern plateau exerts a strong control on the distribution of water vapor (and therefore heat) on the planet by diverting and at times focusing or blocking major atmospheric jets such as the ITCZ and Westerlies (Wallace and Hobbs, 2006; Molnar et al., 2010). Jet diversion around the margins of the plateau affects not only the regional climate, but also areas far downstream, such as in the eastern Mediterranean and Africa (Hoskins and Karoly, 1981; Rodwell and Hoskins, 1996). How sensitive is the climate system to the latitudinal position of the Tibetan

orographic barrier and the distribution of proximal tropical water masses upstream of the jets? Does the location of the steep orographic barrier that may be required to initiate the Indian monsoon (Boos and Kuang, 2010) modulate the seasonal diversion of the ITCZ, intensity of the monsoon, and its teleconnections downstream (Hoskins and Karoly, 1981; Wallace and Hobbs, 2006; Huber and Goldner, 2012)? Did the presence of the Greater India Basin, and therefore tropical throughflow from the Pacific to the subtropical paleo–Arabian Sea and eastern Mediterranean Tethys, enhance the distribution of seasonal precipitation and amplify continental weathering along the margins of these water masses (e.g., Kent and Muttoni, 2008, 2013; Bookhagen et al., 2005)? If there is a strong link between the paleolatitude of the Lhasa-plano, the Greater India Basin, and precipitation patterns in and around Tibet, then we should expect feedbacks with vegetation and erosion, which will in turn alter ocean chemistry (Misra and Froelich, 2012; Pälike et al., 2012), and perhaps even the carbon cycle (France-Lanord and Derry, 1997; Kent and Muttoni, 2008, 2013; Allen and Armstrong, 2012) if physical and chemical erosion rates are high. Prolonged and enhanced seasonal precipitation in Eocene and Oligocene time, fueled in part by the steep and high topographic barrier of the proto-Himalaya and Tibetan Plateau, but also by the presence of the tropical Greater India Basin (and the presence of the para-Tethys in Central Asia (Ramstein et al., 1997; Bosboom et al., 2011), is also expected to have substantially modified the distribution and isotopic composition of precipitation on the proto-Himalaya foreland and Tibetan Plateau. These environmental factors must be considered when interpreting archives of ancient precipitation to infer the paleoaltimetry of Tibet in deep time. From a global perspective, future climate sensitivity studies should explore the direct and secondary effects of a larger, less circuitous tropical seaway on Cenozoic climate change. The possible relationships between the demise of the Greater India Basin, the carbon cycle, and Eocene cooling may be particularly important (Hotinski and Toggweiler, 2003; von der Heydt and Dijkstra, 2008; Zhang et al., 2011).

Evaluating the topographic-atmospheric feedbacks introduced here is well beyond the scope of this study. Our analysis has provided a key boundary condition for climate modelers to incorporate in their simulations of Paleogene Earth, i.e., the paleolatitude of the southern margin of Asia and the proto-Tibetan Plateau.

CONCLUSIONS

Our compilation of diverse paleomagnetic records from the Lhasa terrane has been evaluated in a statistically consistent framework to calculate a paleolatitude record for the southern margin of the terrane since ca. 110 Ma. Our analysis suggests that the southern margin of Asia has remained relatively stable with respect to the Earth's spin axis throughout the Cretaceous and early Paleogene, and has moved northward by ~8° of latitude mostly since 50 Ma. The paleomagnetically estimated collision age between the Tibetan Himalaya and the southern margin

of Asia is ca. 49.5 ± 4.5 Ma, if not a few million years earlier. Adding reasonable estimates for the width of the original Asian forearc, and subducted northern Tibetan Himalayan passive margin rocks may revise this collision age to ca. 52 ± 5 Ma. These age estimates are in excellent agreement with stratigraphic records of this collisional event suggesting a ca. 52 Ma collision. This collision occurred at lat ~21° ± 4°N, or perhaps ~2° lower if a reasonably sized forearc is added. A Tibetan Himalayan–Lhasa collision ca. 52–50 Ma at ~21°N indicates that at most only ~1100 ± 560 km of India-Asia convergence was partitioned into Asian lithosphere. The low end of these paleomagnetic estimates is consistent with the ~740 km of upper crustal shortening within Asia calculated from structural geologic studies (van Hinsbergen et al., 2011a). A direct implication of these findings is that 1700 ± 560 km or more convergence was partitioned into the lower plate (i.e., units of Indian affinity). Thus, Greater India at the time of the Tibetan Himalaya–Lhasa collision was much larger than constrained by pre–Early Cretaceous paleomagnetic data and tectonic reconstructions. As considered elsewhere (van Hinsbergen et al., 2012b), these observations require significant extension of Greater India lithosphere after break-up from Gondwana but prior to collision with the southern margin of Asia. Cretaceous extension within Greater India resulted in the oceanic Greater India Basin, which may have maintained oceanic circulation between the Equatorial Pacific and eastern Mediterranean Tethys throughout most of the Paleogene. The significance of this marine gateway to early Cenozoic climate dynamics and surface processes within the Tethyan realm is beyond the scope of this paper, but we suspect it may be large. Our analysis suggests that the southern margin of the Tibetan Plateau has been positioned at high tropical to low subtropical latitudes since at least the end of Early Cretaceous. Future climate model simulations should incorporate this paleogeography to more accurately explore how atmospheric processes interact with or are modified by the high uniform topography of the Tibetan Plateau. Teleconnections between atmospheric jets, regional precipitation patterns, and the long-term carbon cycle may be particularly sensitive to the paleolatitude of orogenic plateaus.

ACKNOWLEDGMENTS

REFERENCES CITED

Achache, J., Courtillot, V., and Zhou, Y.X., 1984, Paleogeographic and tectonic evolution of southern Tibet since middle Cretaceous time: New paleomagnetic data and synthesis: Journal of Geophysical Research, v. 89, p. 311–339, doi:10.1029/JB089iB12p10311.

Agard, P., Omrani, J., Jolivet, L., Whitechurch, H., Vrielynck, B., Spakman, W., Monie, P., Meyer, B., and Wortel, R., 2011, Zagros orogeny: A subduction-dominated process: Geological Magazine, v. 148, p. 692–725, doi:10.1017/S001675681100046X.

Aitchison, J.C., Ali, J.R., and Davis, A.M., 2007, When and where did India and Asia collide?: Journal of Geophysical Research, v. 112, doi:10.1029/2006JB004706.

Ali, J.R., and Aitchison, J.C., 2004, Problem of positioning Paleogene Eurasia: A review. Efforts to resolve the issue and implications for the India-Asia collision, *in* Clift, P.D., ed., Continent-Ocean Interactions within East Asian Marginal Seas: American Geophysical Union Geophysical Monograph 149, p. 23–35, doi:10.1029/149GM02.

Ali, J.R., and Aitchison, J.C., 2006, Positioning Paleogene Eurasia problem: Solution for 60–50 Ma and broader tectonic implications: Earth and Planetary Science Letters, v. 251, p. 148–155, doi:10.1016/j.epsl.2006.09.003.

Allen, M.B., and Armstrong, H.A., 2012, Reconciling the Intertropical Convergence Zone, Himalayan/Tibetan tectonics, and the onset of the Asian monsoon system: Journal of Asian Earth Sciences, v. 44, p. 36–47, doi:10.1016/j.jseaes.2011.04.018.

Allen, M., Jackson, J., and Walker, R., 2004, Late Cenozoic reorganization of the Arabia-Eurasia collision and the comparison of short-term and long-term deformation rates: Tectonics, v. 23, TC2008, doi:10.1029/2003tc001530.

Appel, E., and Li, H.M., 1988, The northern edge of the Indian Plate from Albian to Paleocene, *in* Himalaya-Tibet-Karakorum Workshop Meeting Proceedings: Lausanne, Switzerland, Musee Cantonal de Geologie, Instituts de Geologie et de Mineralogie de l'Unil, p. 10.

Arason, P., and Levi, S., 2010, Maximum likelihood solution for inclination-only data in paleomagnetism: Geophysical Journal International, v. 182, p. 753–771, doi:10.1111/j.1365-246X.2010.04671.x.

Argnani, A., 2012, Plate motion and the evolution of Alpine Corsica and Northern Apennines: Tectonophysics, v. 579, p. 207–219, doi:10.1016/j.tecto.2012.06.010.

Besse, J., Courtillot, V., Pozzi, J.P., Westphal, M., and Zhou, Y.X., 1984, Paleomagnetic estimates of crustal shortening in the Himalayan thrusts and Zangbo suture: Nature, v. 311, p. 621–626, doi:10.1038/311621a0.

Biggin, A.J., van Hinsbergen, D.J.J., Langereis, C.G., Straathof, G.B., and Deenen, M.H.L., 2008, Geomagnetic secular variation in the Cretaceous Normal Superchron and in the Jurassic: Physics of the Earth and Planetary Interiors, v. 169, p. 3–19, doi:10.1016/j.pepi.2008.07.004.

Bookhagen, B., Theide, R.C., and Strecker, M.R., 2005, Abnormal monsoon years and their control on erosion and sediment flux in the high, arid northwest Himalaya: Earth and Planetary Science Letters, v. 231, p. 131–146, doi:10.1016/j.epsl.2004.11.014.

Boos, W.R., and Kuang, Z.M., 2010, Dominant control of the South Asian monsoon by orographic insulation versus plateau heating: Nature, v. 463, p. 218–222, doi:10.1038/nature08707.

Bosboom, R.E., Dupont-Nivet, G., Houben, A.J.P., Brinkhuis, H., Villa, G., Mandic, O., Stoica, M., Zachariasse, W., Guo, Z., Li, C., and Krijgsman, W., 2011, Late Eocene sea retreat from the Tarim Basin (west China) and concomitant Asian paleoenvironmental change: Palaeogeography, Palaeoclimatology, Palaeoecology, v. 299, p. 385–398, doi:10.1016/j.palaeo.2010.11.019.

Butler, R.F., 1992, Paleomagnetism: Magnetic Domains to Geologic Terranes: Malden, Massachusetts, Blackwell Scientific, 238 p.

Cande, S.C., and Kent, D.V., 1995, Revised calibration of the geomagnetic polarity timescale for the Late Cretaceous and Cenozoic: Journal of Geophysical Research, v. 100, p. 6093–6095, doi:10.1029/94JB03098.

Cande, S.C., and Stegman, D.R., 2011, Indian and African plate motions driven by the push force of the Reunion plume head: Nature, v. 475, p. 47–52, doi:10.1038/nature10174.

Capitanio, F.A., Morra, G., Goes, S., Weinberg, R.F., and Moresi, L., 2010, India-Asia convergence driven by the subduction of the Greater Indian continent: Nature Geoscience, v. 3, p. 136–139, doi:10.1038/ngeo725.

Chemenda, A.I., Burg, J.P., and Mattauer, M., 2000, Evolutionary model of the Himalaya-Tibet system: Geopoem based on new modelling, geological

and geophysical data: Earth and Planetary Science Letters, v. 174, p. 397–409, doi:10.1016/S0012-821X(99)00277-0.

Chen, J.S., Huang, B.C., and Sun, L.S., 2010, New constraints to the onset of the India-Asia collision: Paleomagnetic reconnaissance of the Linzizong Group in the Lhasa Block, China: Tectonophysics, v. 489, p. 189–209, doi:10.1016/j.tecto.2010.04.024.

Chen, W., Yang, T., Zhang, S., Yang, Z., Li, H., Wu, H., Zhang, J., Ma, Y., and Cai, F., 2012, Paleomagnetic results from the Early Cretaceous Zenong Group volcanic rocks, Cuoqin, Tibet, and their paleogeographic implications: Gondwana Research, v. 22, p. 461–469, doi:10.1016/j.gr.2011.07.019.

Chen, Y., Courtillot, V., Cogné, J.P., Besse, J., Yang, Z.Y., and Enkin, R., 1993, The configuration of Asia prior to the collision of India: Cretaceous paleomagnetic constraints: Journal of Geophysical Research, v. 98, p. 21927–21941, doi:10.1029/93JB02075.

Clark, M.K., 2012, Continental collision slowing due to viscous mantle lithosphere rather than topography: Nature, v. 483, p. 74–77, doi:10.1038/nature10848.

Cogné, J.P., Halim, N., Chen, Y., and Courtillot, V., 1999, Resolving the problem of shallow magnetization of Tertiary age in Asia: Insights from paleomagnetic data from the Qiangtang, Kunlun, and Qaidam blocks (Tibet, China), and a new hypothesis: Journal of Geophysical Research, v. 104, p. 17715–17734, doi:10.1029/1999JB900153.

Cogné, J.P., Besse, J., Chen, Y., and Hankard, F., 2013, A new Late Cretaceous to present APWP for Asia and its implications for paleomagnetic shallow inclinations in Central Asia and Cenozoic Eurasian plate deformation: Geophysical Journal International, v. 192, p. 1000–1024, doi:10.1093/gji/ggs104.

Copley, A., Avouac, J.P., and Royer, J.Y., 2010, The India-Asia collision and the Cenozoic slowdown of the Indian plate: Implications for the forces driving plate motions: Journal of Geophysical Research, v. 115, B03410, doi:10.1029/2009JB006634.

Copley, A., Avouac, J.-P., and Wernicke, B.P., 2011, Evidence for mechanical coupling and strong Indian lower crust beneath southern Tibet: Nature, v. 472, p. 79–81, doi:10.1038/nature09926.

Cox, A., and Hart, R.B., 1986, Plate Tectonics: How It Works: Cambridge, Massachusetts, Blackwell Science, 392 p.

DeCelles, P.G., Robinson, D.M., and Zandt, G., 2002, Implications of shortening in the Himalayan fold-thrust belt for uplift of the Tibetan Plateau: Tectonics, v. 21, no. 6, p. 12-1–12-25, doi:10.1029/2001TC001322.

DeCelles, P.G., Kapp, P., Ding, L., and Gehrels, G.E., 2007, Late Cretaceous to middle Tertiary basin evolution in the central Tibetan Plateau: Changing environments in response to tectonic partitioning, aridification, and regional elevation gain: Geological Society of America Bulletin, v. 119, p. 654–680, doi:10.1130/B26074.1.

Deenen, M.H.L., Langereis, C.G., van Hinsbergen, D.J.J., and Biggin, A.J., 2011, Geomagnetic secular variation and the statistics of palaeomagnetic directions: Geophysical Journal International, v. 186, p. 509–520, doi:10.1111/j.1365-246X.2011.05050.x.

Dettman, D.L., Fang, X.M., Garzione, C.N., and Li, J.J., 2003, Uplift-driven climate change at 12 Ma: A long $\delta^{18}O$ record from the NE margin of the Tibetan plateau: Earth and Planetary Science Letters, v. 214, p. 267–277, doi:10.1016/S0012-821X(03)00383-2.

Dewey, J.F., Cande, S.C., and Pitman, W.C., 1989, Tectonic evolution of the India-Eurasia collision zone: Eclogae Geologicae Helvetiae, v. 82, p. 717–734.

Ding, L., Kapp, P., and Wan, X.Q., 2005, Paleocene–Eocene record of ophiolite obduction and initial India-Asia collision, south central Tibet: Tectonics, v. 24, TC3001, doi:10.1029/2004TC001729.

Ding, L., Kapp, P., Yue, Y.H., and Lai, Q.Z., 2007, Postcollisional calc-alkaline lavas and xenoliths from the southern Qiangtang terrane, central Tibet: Earth and Planetary Science Letters, v. 254, p. 28–38, doi:10.1016/j.epsl.2006.11.019.

Doubrovine, P.V., and Tarduno, J.A., 2008, Linking the Late Cretaceous to Paleogene Pacific plate and the Atlantic bordering continents using plate circuits and paleomagnetic data: Journal of Geophysical Research, v. 113, B07104, doi:101029/2008JB005564.

Dupont-Nivet, G., Hoorn, C., and Konert, M., 2008, Tibetan uplift prior to the Eocene–Oligocene climate transition: Evidence from pollen analysis of the Xining Basin: Geology, v. 36, p. 987–990, doi:10.1130/G25063A.1.

Dupont-Nivet, G., Lippert, P.C., van Hinsbergen, D.J.J., Meijers, M.J.M., and Kapp, P., 2010a, Palaeolatitude and age of the Indo-Asia collision:

Palaeomagnetic constraints: Geophysical Journal International, v. 182, p. 1189–1198, doi:10.1111/j.1365-246X.2010.04697.x.

Dupont-Nivet, G., van Hinsbergen, D.J.J., and Torsvik, T.H., 2010b, Persistently low Asian paleolatitudes: Implications for the Indo-Asian collision history: Tectonics, v. 29, doi:10.1029/2008TC002437.

Einsele, G., Liu, B., Dürr, S., Frisch, W., Liu, G., Luterbacher, H.P., Ratschbacher, L., Ricken, W., Wendt, J., Wetzel, A., Yu, G., and Zheng, H., 1994, The Xigaze forearc basin: Evolution and facies architecture (Cretaceous, Tibet): Sedimentary Geology, v. 90, p. 1–32, doi:10.1016/0037-0738(94)90014-0.

England, P., and Houseman, G., 1986, Finite strain calculations of continental deformation 2: Comparison with the India-Asia collision zone: Journal of Geophysical Research, v. 91, p. 3664–3676, doi:10.1029/JB091iB03p03664.

England, P.C., and Searle, M.P., 1986, The Cretaceous–Tertiary deformation of the Lhasa block and its implications for crustal thickening in Tibet: Tectonics, v. 5, p. 1–14, doi:10.1029/TC005i001p00001.

Fisher, R.A., 1953, Dispersion on a sphere: Royal Society of London Proceedings, ser. A, v. 217, p. 295–305, doi:10.1098/rspa.1953.0064.

Flesch, L.M., Holt, W.E., Silver, P.G., Stephenson, M., Wang, C.Y., and Chan, W.W., 2005, Constraining the extent of crust-mantle coupling in central Asia using GPS, geologic, and shear wave splitting data: Earth and Planetary Science Letters, v. 238, p. 248–268, doi:10.1016/j.epsl.2005.06.023.

France-Lanord, C., and Derry, L.A., 1997, Organic carbon burial forcing of the carbon cycle from Himalayan erosion: Nature, v. 390, p. 65–67, doi:10.1038/36324.

Gaina, C., Torsvik, T.H., van Hinsbergen, D.J.J., Medvedev, S., Werner, S.C., and Labails, C., 2013, The African plate: A history of oceanic crust accretion and subduction since the Jurassic: Tectonophysics, v. 604, p. 4–25, doi:10.1016/j.tecto.2013.05.037.

Garzanti, E., 1999, Stratigraphy and sedimentary history of the Nepal Tethys Himalaya passive margin: Journal of Asian Earth Sciences, v. 17, p. 805–827, doi:10.1016/S1367-9120(99)00017-6.

Gilder, S.A., Chen, Y., and Sen, S., 2001, Oligo-Miocene magnetostratigraphy and environmental magnetism of the Xishuigou section, Subei (Gansu Province, western China): Further implication on the shallow inclination of central Asia: Journal of Geophysical Research, v. 106, p. 30505–30521, doi:10.1029/2001JB000325.

Gradstein, F.M., Agterberg, F.P., Ogg, J.G., Hardenbol, J., van Veen, P., Thierry, J., and Huang, Z., 1994, A Mesozoic time scale: Journal of Geophysical Research, v. 99, p. 24,051–024,074, doi:10.1029/94JB01889.

Green, O.R., Searle, M.P., Corfield, R.I., and Corfield, R.M., 2008, Cretaceous–Tertiary carbonate platform evolution and the age of the India-Asia collision along the Ladakh Himalaya (northwest India): Journal of Geology, v. 116, p. 331–353, doi:10.1086/588831.

Hall, R., 2012, Late Jurassic–Cenozoic reconstructions of the Indonesian region and the Indian Ocean: Tectonophysics, v. 570–571, p. 1–41, doi:10.1016/j.tecto.2012.04.021.

Hankard, F., Cogné, J.P., Kravchinsky, V., Carporzen, L., Bayasgalan, A., and Lkhagvadorj, P., 2007, New Tertiary paleomagnetic poles from Mongolia and Siberia at 40, 30, 20, and 13 Ma: Clues on the inclination shallowing problem in Central Asia: Journal of Geophysical Research, v. 112, B02101, doi:10.1029/2006JB004488.

He, S.D., Kapp, P., DeCelles, P.G., Gehrels, G.E., and Heizler, M., 2007, Cretaceous–Tertiary geology of the Gangdese Arc in the Linzhou area, southern Tibet: Tectonophysics, v. 433, p. 15–37, doi:10.1016/j.tecto.2007.01.005.

Hébert, R., Bezard, R., Guilmette, C., Dostal, J., Wang, C.S., and Liu, Z.F., 2012, The Indus-Yarlung Zangbo ophiolites from Nanga Parbat to Namche Barwa syntaxes, southern Tibet: First synthesis of petrology, geochemistry, and geochronology with incidences on geodynamic reconstructions of Neo-Tethys: Gondwana Research, v. 22, p. 377–397, doi:10.1016/j.gr.2011.10.013.

Hodges, K.V., 2000, Tectonics of the Himalaya and southern Tibet from two perspectives: Geological Society of America Bulletin, v. 112, p. 324–350, doi:10.1130/0016-7606(2000)112<324:TOTHAS>2.0.CO;2.

Horton, B.K., Yin, A., Spurlin, M.S., Zhou, J.Y., and Wang, J.H., 2002, Paleocene–Eocene syncontractional sedimentation in narrow, lacustrine-dominated basins of east-central Tibet: Geological Society of America Bulletin, v. 114, p. 771–786, doi:10.1130/0016-7606(2002)114<0771:PESSIN>2.0.CO;2.

Horton, B.K., Dupont-Nivet, G., Zhou, J., Waanders, G.L., Butler, R.F., and Wang, J., 2004, Mesozoic–Cenozoic evolution of the Xining-Minhe and

Early Cretaceous–present latitude of the proto-Tibetan Plateau

Dangchang basins, northeastern Tibetan Plateau: Magnetostratigraphic and biostratigraphic results: Journal of Geophysical Research, v. 109, doi: 10.1029/2003JB002913.

Hoskins, B.J., and Karoly, D.J., 1981, The steady linear response of a spherical atmosphere to thermal and orographic forcing: Journal of the Atmospheric Sciences, v. 38, p. 1179–1196, doi:10.1175/1520-0469(1981)038 <1179:TSLROA>2.0.CO;2.

Hotinski, R.M., and Toggweiler, J.R., 2003, Impact of a Tethyan circumglobal passage on ocean heat transport and "equable" climates: Paleoceanography, v. 18, 1007, doi:10.1029/2001PA000730.

Hough, B.G., Garzione, C.N., Wang, Z., Lease, R.O., Burbank, D.W., and Yuan, D., 2011, Stable isotope evidence for topographic growth and basin segmentation: Implications for the evolution of the NE Tibetan Plateau: Geological Society of America Bulletin, v. 123, p. 168–185, doi:10.1130 /B30090.1.

Hsu, K.J., Pan, G.T., and Sengor, A.M.C., 1995, Tectonic evolution of the Tibetan plateau: A working hypothesis based on the archipelago model of orogenesis: International Geology Review, v. 37, p. 473–508, doi:10.1080 /00206819509465414.

Hu, X.M., Sinclair, H.D., Wang, J.G., Jiang, H.H., and Wu, F.Y., 2012, Late Cretaceous–Palaeogene stratigraphic and basin evolution in the Zhepure Mountain of southern Tibet: Implications for the timing of India-Asia initial collision: Basin Research, v. 24, p. 520–543, doi:10.1111/j.1365-2117 .2012.00543.x.

Huber, M., and Goldner, A., 2012, Eocene monsoons: Journal of Asian Earth Sciences, v. 44, p. 3–23, doi:10.1016/j.jseaes.2011.09.014.

Iaffaldano, G., and Bunge, H.P., 2009, Relating rapid plate-motion variations to plate-boundary forces in global coupled models of the mantle/lithosphere system: Effects of topography and friction: Tectonophysics, v. 474, p. 393–404, doi:10.1016/j.tecto.2008.10.035.

Iaffaldano, G., Bunge, H.P., and Bucker, M., 2007, Mountain belt growth inferred from histories of past plate convergence: A new tectonic inverse problem: Earth and Planetary Science Letters, v. 260, p. 516–523, doi:10 .1016/j.epsl.2007.06.006.

Ji, W.-Q., Wu, F.-Y., Chung, S.-L., Li, J.-X., and Liu, C.-Z., 2009, Zircon U-Pb geochronology and Hf isotopic constraints on petrogenesis of the Gangdese batholith, southern Tibet: Chemical Geology, v. 262, p. 229–245, doi:10.1016/j.chemgeo.2009.01.020.

Johnson, C.L., Constable, C.G., Tauxe, L., Barendregt, R., Brown, L.L., Coe, R.S., Layer, P., Mejia, V., Opdyke, N., Singers, B., Staudigel, H., and Stone, D., 2008, Recent investigations of the 0–5 Ma geomagnetic field recorded by lava flows: Geochemistry Geophysics Geosystems, v. 9, doi: 10.1029/2007GC001696.

Jolivet, M., Brunel, M., Seward, D., Xu, Z., Yang, J., Roger, F., Tapponnier, P., Malavieille, J., Arnaud, N., and Wu, C., 2001, Mesozoic and Cenozoic tectonics of the northern edge of the Tibetan plateau: Fission-track constraints: Tectonophysics, v. 343, p. 111–134, doi:10.1016/S0040-1951 (01)00196-2.

Kapp, P., Yin, A., Harrison, T.M., and Ding, L., 2005, Cretaceous–Tertiary shortening, basin development, and volcanism in central Tibet: Geological Society of America Bulletin, v. 117, p. 865–878, doi:10.1130/B25595.1.

Kapp, P., DeCelles, P.G., Gehrels, G.E., Heizler, M., and Ding, L., 2007a, Geological records of the Lhasa-Qiangtang and Indo-Asian collisions in the Nima area of central Tibet: Geological Society of America Bulletin, v. 119, p. 917–933, doi:10.1130/B26033.1.

Kapp, P., DeCelles, P.G., Leier, A.L., Fabijanic, J.M., He, S., Pullen, A., Gehrels, G.E., and Ding, L., 2007b, The Gangdese retroarc thrust belt revealed: GSA Today, v. 17, no. 7, p. 4–9, doi:10.1130/GSAT01707A.1.

Kent, D.V., and Muttoni, G., 2008, Equatorial convergence of India and early Cenozoic climate trends: National Academy of Sciences Proceedings, v. 105, p. 16065–16070, doi:10.1073/pnas.0805382105.

Kent, D.V., and Muttoni, G., 2013, Modulation of Late Cretaceous and Cenozoic climate by variable drawdown of atmospheric pCO2 from weathering of basaltic provinces on continents drifting through the equatorial humid belt: Climate of the Past, v. 9, no. 2, p. 525–546, doi:10.5194/cp-9-525-2013.

King, R.F., 1955, The remanent magnetism of artificially deposited sediments: Geophysical Journal International, v. 7, supplement 3, p. 115–134, doi:10 .1111/j.1365-246X.1955.tb06558.x.

Kirby, E., Reiners, P.W., Krol, M.A., Whipple, K.X., Hodges, K.V., Farley, K.A., Tang, W., and Chen, Z., 2002, Late Cenozoic evolution of the eastern margin of the Tibetan plateau: Inferences from ^{40}Ar/^{39}Ar and (U-Th)/He thermochronology: Tectonics, v. 21, doi:10.1029/2000TC001246.

Klootwijk, C.T., Gee, J.S., Peirce, J.W., Smith, G.M., and McFadden, P.L., 1992, An early India-Asia contact: Paleomagnetic constraints from Ninetyeast Ridge, ODP Leg 121: Geology, v. 20, p. 395–398, doi:10.1130 /0091-7613(1992)020<0395:AEIACP>2.3.CO;2.

Kodama, K.P., 2009, Simplification of the anisotropy-based inclination correction technique for magnetite- and haematite-bearing rocks: A case study for the Carboniferous Glenshaw and Mauch Chunk Formations, North America: Geophysical Journal International, v. 176, p. 467–477, doi:10 .1111/j.1365-246X.2008.04013.x.

Lease, R.O., Burbank, D.W., Hough, B., Wang, Z., and Yuan, D., 2012, Pulsed Miocene range growth in northeastern Tibet: Insights from Xunhua Basin magnetostratigraphy and provenance: Geological Society of America Bulletin, v. 124, p. 657–677, doi:10.1130/B30524.1.

Lee, H.Y., Chung, S.L., Lo, C.H., Ji, J.Q., Lee, T.Y., Qian, Q., and Zhang, Q., 2009, Eocene Neotethyan slab breakoff in southern Tibet inferred from the Linzizong volcanic record: Tectonophysics, v. 477, p. 20–35, doi:10 .1016/j.tecto.2009.02.031.

Leier, A.L., DeCelles, P.G., Kapp, P., and Ding, L., 2007a, The Takena Formation of the Lhasa terrane, southern Tibet: The record of a Late Cretaceous retroarc foreland basin: Geological Society of America Bulletin, v. 119, p. 31–48, doi:10.1130/B25974.1.

Leier, A.L., Kapp, P., Gehrels, G.E., and DeCelles, P.G., 2007b, Detrital zircon geochronology of Carboniferous–Cretaceous strata in the Lhasa terrane, southern Tibet: Basin Research, v. 19, p. 361–378, doi:10.1111/j.1365 -2117.2007.00330.x.

Liebke, U., Appel, E., Ding, L., Neumann, U., Antolin, B., and Xu, Q.A., 2010, Position of the Lhasa terrane prior to India-Asia collision derived from palaeomagnetic inclinations of 53 Ma old dykes of the Linzhou Basin: Constraints on the age of collision and post-collisional shortening within the Tibetan Plateau: Geophysical Journal International, v. 182, p. 1199–1215, doi:10.1111/j.1365-246X.2010.04698.x.

Liebke, U., Appel, E., Neumann, U., and Ding, L., 2012, Dual polarity directions in basaltic-andesitic dykes—Reversal record or self-reversed magnetization?: Geophysical Journal International, v. 190, p. 887–899, doi:10 .1111/j.1365-246X.2012.05543.x.

Lin, J., and Watts, D.R., 1988, Paleomagnetic results from the Tibetan Plateau: Royal Society of London Philosophical Transactions, ser. A, v. 327, p. 239–262, doi:10.1098/rsta.1988.0128.

Linder, J., and Gilder, S.A., 2012, Latitude dependency of the geomagnetic secular variation S parameter: A mathematical artifact: Geophysical Research Letters, v. 39, L02308, doi:10.1029/2011GL050330.

Lippert, P.C., Zhao, X.X., Coe, R.S., and Lo, C.H., 2011, Paleomagnetism and ^{40}Ar/^{39}Ar geochronology of upper Paleogene volcanic rocks from central Tibet: Implications for the Central Asia inclination anomaly, the paleolatitude of Tibet, and post-50 Ma shortening within Asia: Geophysical Journal International, v. 184, p. 131–161, doi:10.1111/j.1365-246X.2010.04833.x.

Liu, H., 1993, Classification and age attribution of the Linzizong volcanic series in the Lhasa area of Tibet: Tibetan Geology, v. 10, p. 59–68.

Long, S., McQuarrie, N., Tobgay, T., and Grujic, D., 2011, Geometry and crustal shortening of the Himalayan fold-thrust belt, eastern and central Bhutan: Geological Society of America Bulletin, v. 123, p. 1427–1447, doi:10.1130/B30203.1.

Lovlie, R., and Torsvik, T., 1984, Magnetic remanence and fabric properties of laboratory deposited hematite bearing red sandstone: Geophysical Research Letters, v. 11, p. 221–229, doi:10.1029/GL011i003p00221.

Maluski, H., Proust, F., and Xiao, X.C., 1982, ^{39}Ar/^{40}Ar dating of the transHimalayan calc-alkaline magmatism of southern Tibet: Nature, v. 298, p. 152–154, doi:10.1038/298152a0.

Manabe, S., and Terpstra, T., 1974, The effects of mountains on the general circulation of the atmosphere as identified by numerical experiments: Journal of the Atmospheric Sciences, v. 31, p. 3–42, doi:10.1175/1520-0469 (1974)031<0003:TEOMOT>2.0.CO;2.

Mankinen, E.A., Prevot, M., Gromme, C.G., and Coe, R.S., 1985, The Steens Mountain (Oregon) geomagnetic polarity transition 1. Directional history, duration of episodes, and rock magnetism: Journal of Geophysical Research, v. 90, p. 10393–10416, doi:10.1029/JB090iB12p10393.

McFadden, P.L., 1990, A new fold test for palaeomagnetic studies: Geophysical Journal International, v. 103, p. 163–169, doi:10.1111/j.1365-246X.1990 .tb01761.x.

McFadden, P.L., and McElhinny, M.W., 1990, Classification of the reversal test in palaeomagnetism: Geophysical Journal International, v. 103, p. 725–729, doi:10.1111/j.1365-246X.1990.tb05683.x.

Misra, S., and Froelich, P.N., 2012, Lithium isotope history of Cenozoic seawater: Changes in silicate weathering and reverse weathering: Science, v. 335, p. 818–823, doi:10.1126/science.1214697.

Mo, X., Niu, Y., Dong, G., Zhao, Z., Hou, Z., Zhou, S., and Ke, S., 2008, Contribution of syncollisional felsic magmatism to continental crust growth: A case study of the Paleogene Linzizong volcanic succession in southern Tibet: Chemical Geology, v. 250, p. 49–67, doi:10.1016/j.chemgeo.2008.02.003.

Molnar, P., and Lyon-Caen, H., 1988, Some simple physical aspects of the support, structure, and evolution of mountain belts, *in* Clark, S.P., et al., eds., Processes in Continental Lithospheric Deformation: Geological Society of America Special Paper 218, p. 179–208, doi:10.1130/SPE218-p179.

Molnar, P., and Stock, J.M., 2009, Slowing of India's convergence with Eurasia since 20 Ma and its implication for Tibetan mantle dynamics: Tectonics, v. 28, TC3001, doi:10.1029/2008TC002271.

Molnar, P., and Tapponnier, P., 1975, Cenozoic tectonics of Asia: Effects of a continental collision: Science, v. 189, p. 419–426, doi:10.1126/science.189.4201.419.

Molnar, P., Boos, W.R., and Battisti, D.S., 2010, Orographic controls on climate and paleoclimate of Asia: Thermal and mechanical roles for the Tibetan Plateau: Annual Review of Earth and Planetary Sciences, v. 38, p. 77–102, doi:10.1146/annurev-earth-040809-152456.

Müller, R.D., Sdrolias, M., Gaina, C., Steinberger, B., and Heine, C., 2008, Long-term sea-level fluctuations driven by ocean basin dynamics: Science, v. 319, p. 1357–1362, doi:10.1126/science.1151540.

Murphy, M.A., and Yin, A., 2003, Structural evolution and sequence of thrusting in the Tethyan fold-thrust belt and Indus-Yalu suture zone, southwest Tibet: Geological Society of America Bulletin, v. 115, p. 21–34, doi:10.1130/0016-7606(2003)115<0021:SEASOT>2.0.CO;2.

Murphy, M.A., Yin, A., Harrison, T.M., Durr, S.B., Chen, Z., Ryerson, F.J., Kidd, W.S.F., Wang, X., and Zhou, X., 1997, Did the Indo-Asian collision alone create the Tibetan plateau?: Geology, v. 25, p. 719–722, doi:10.1130/0091-7613(1997)025<0719:DTIACA>2.3.CO;2.

Najman, Y., Appel, E., Boudagher-Fadel, M., Bown, P., Carter, A., Garzanti, E., Godin, L., Han, J., Liebke, U., Oliver, G., Parrish, R., and Vezzoli, G., 2010, The timing of India-Asia collision: Geological, biostratigraphic and paleomagnetic constraints: Journal of Geophysical Research, v. 115, B12416, doi:10.1029/2010JB007673.

Oncken, O., Hindle, D., Kley, J., Elger, K., Victor, P., and Schemmann, K., 2006, Deformation of the Central Andean upper plate system—Facts, fiction, and constraints for plateau models, *in* Oncken, O., et al., eds., The Andes: Berlin, Springer, p. 3–27.

Pälike, H., and 64 others, 2012, A Cenozoic record of the equatorial Pacific carbonate compensation depth: Nature, v. 488, p. 609–614, doi:10.1038/nature11360.

Patzelt, A., Li, H.M., Wang, J.D., and Appel, E., 1996, Palaeomagnetism of Cretaceous to Tertiary sediments from southern Tibet: Evidence for the extent of the northern margin of India prior to the collision with Eurasia: Tectonophysics, v. 259, p. 259–284, doi:10.1016/0040-1951(95)00181-6.

Pozzi, J.P., Westphal, M., Zhou, Y.X., Xing, L.S., and Chen, Z.Y., 1982, Position of the Lhasa block, South Tibet, during the Late Cretaceous: Nature, v. 297, p. 319–321, doi:10.1038/297319a0.

Pullen, A., Kapp, P., Gehrels, G.E., DeCelles, P.G., Brown, E.H., Fabijanic, J.M., and Ding, L., 2008, Gangdese retroarc thrust belt and foreland basin deposits in the Damxung area, southern Tibet: Journal of Asian Earth Sciences, v. 33, p. 323–336, doi:10.1016/j.jseaes.2008.01.005.

Quade, J., Breecker, D.O., Daeron, M., and Eiler, J., 2011, The paleoaltimetry of Tibet: An isotopic perspective: American Journal of Science, v. 311, p. 77–115, doi:10.2475/02.2011.01.

Ramstein, G., Fluteau, F., Besse, J., and Joussaume, S., 1997, Effect of orogeny, plate motion and land-sea distribution on Eurasian climate change over the past 30 million years: Nature, v. 386, p. 788–795, doi:10.1038/386788a0.

Ratschbacher, L., Frisch, W., Chen, C., and Pan, G., 1994, Distributed deformation in southern and western Tibet during and after the India-Asian collision: Journal of Geophysical Research, v. 99, p. 19917–19945, doi:10.1029/94JB00932.

Richardson, N.J., Densmore, A.L., Seward, D., Fowler, A., Wipf, M., Ellis, M.A., Yong, L., and Zhang, Y., 2008, Extraordinary denudation in the Sichuan Basin: Insights from low-temperature thermochronology adjacent to the eastern margin of the Tibetan Plateau: Journal of Geophysical Research, v. 113, p. 1–23, doi:10.1029/2006JB004739.

Rodwell, M.J., and Hoskins, B.J., 1996, Monsoons and the dynamics of deserts: Royal Meteorological Society Quarterly Journal, v. 122, p. 1385–1404, doi:10.1002/qj.49712253408.

Rohrmann, A., Kapp, P., Carrapa, B., Reiners, P.W., Guynn, J., Ding, L., and Heizler, M., 2012, Thermochronologic evidence for plateau formation in central Tibet by 45 Ma: Geology, v. 40, p. 187–190, doi:10.1130/G32530.1.

Rowley, D.B., 1996, Age of initiation of collision between India and Asia: A review of stratigraphic data: Earth and Planetary Science Letters, v. 145, p. 1–13, doi:10.1016/S0012-821X(96)00201-4.

Roy, S.S., 1976, A possible Himalayan microcontinent: Nature, v. 263, p. 117–120, doi:10.1038/263117a0.

Royden, L.H., Burchfiel, B.C., and van der Hilst, R.D., 2008, The geological evolution of the Tibetan Plateau: Science, v. 321, p. 1054–1058, doi:10.1126/science.1155371.

Searle, M.P., Elliott, J.R., Phillips, R.J., and Chung, S.-L., 2011, Crustal-lithospheric structure and continental extrusion of Tibet: Journal of the Geological Society, v. 168, p. 633–672, doi:10.1144/0016-76492010-139.

Sengör, A.M.C., Özeren, M.S., Keskin, M., Sakinc, M., Özbakir, A.D., and Kayan, I., 2008, Eastern Turkish high plateau as a small Turkic-type orogen: Implications for post-collisional crust-forming processes in Turkic-type orogens: Earth-Science Reviews, v. 90, p. 1–48, doi:10.1016/j.earscirev.2008.05.002.

Si, J., and van der Voo, R., 2001, Too-low magnetic inclinations in central Asia: An indication of long-term Tertiary non-dipole field?: Terra Nova, v. 13, p. 471–478, doi:10.1046/j.1365-3121.2001.00383.x.

Sobel, E.R., Hilley, G.E., and Strecker, M.R., 2003, Formation of internally-drained contractional basins by aridity-limited bedrock incision: Journal of Geophysical Research, v. 108, p. 2344, doi:10.1029/2002JB001883.

Sun, Z., Pei, J., Li, H., Xu, W., Jiang, W., Zhu, Z., Wang, X., and Yang, Z., 2012, Palaeomagnetism of late Cretaceous sediments from southern Tibet: Evidence for the consistent palaeolatitudes of the southern margin of Eurasia prior to the collision with India: Gondwana Research, v. 21, p. 53–63, doi:10.1016/j.gr.2011.08.003.

Sun, Z.M., Jiang, W., Pei, J.L., and Li, H.B., 2008, New Early Cretaceous paleomagnetic data from volcanic of the eastern Lhasa Block and its tectonic implications: Acta Petrolei Sinica, v. 24, p. 1621–1626.

Sun, Z.M., Wan, J., Li, H.B., Pei, J.L., and Zhu, Z.M., 2010, New paleomagnetic results of Paleocene volcanic rocks from the Lhasa block: Tectonic implications for the collision of India and Asia: Tectonophysics, v. 490, p. 257–266, doi:10.1016/j.tecto.2010.05.011.

Tan, X.D., Gilder, S.A., Kodama, K.P., Jiang, W., Han, Y.L., Zhang, H., Xu, H., and Zhou, D., 2010, New paleomagnetic results from the Lhasa block: Revised estimation of latitudinal shortening across Tibet and implications for dating the India-Asia collision: Earth and Planetary Science Letters, v. 293, p. 396–404, doi:10.1016/j.epsl.2010.03.013.

Tapponnier, P., Peltzer, G., Le Dain, Y., Armijo, R., and Cobbold, P.R., 1982, Propagating extrusion tectonics in Asia: New insights from simple experiments with plasticine: Geology, v. 10, p. 611–616, doi:10.1130/0091-7613(1982)10<611:PETIAN>2.0.CO;2.

Tapponnier, P., Xu, Z.Q., Roger, F., Meyer, B., Arnaud, N.O., Wittlinger, G., and Yang, J., 2001, Oblique stepwise rise and growth of the Tibet Plateau: Science, v. 294, p. 1671–1677, doi:10.1126/science.105978.

Tauxe, L., and Kent, D.V., 2004, A simplified statistical model for the geomagnetic field and the detection of shallow bias in paleomagnetic inclinations: Was the ancient field dipolar?, *in* Channell, J.E.T., et al., eds., Timescales of the Paleomagnetic Field: American Geophysical Union Geophysical Monograph 145, p. 101–115, doi:10.1029/145GM08.

Torsvik, T.H., Van der Voo, R., Preeden, U., Mac Niocaill, C., Steinberger, B., Doubrovine, P.V., Van Hinsbergen, D., Domeier, M., Gaina, C., Tohver, E., Meert, J.G., McCausland, P., and Cocks, L., 2012, Phanerozoic polar wander, palaeogeography and dynamics: Earth-Science Reviews, v. 114, p. 325–368, doi:10.1016/j.earscirev.2012.06.007.

Turcotte, D.L., and Schubert, G., 2002, Geodynamics (second edition): Cambridge, UK, Cambridge University Press, 456 p.

Vandamme, D., 1994, A new method to determine paleosecular variation: Physics of the Earth and Planetary Interiors, v. 85, p. 131–142, doi:10.1016/0031-9201(94)90012-4.

van der Voo, R., 1990, The reliability of paleomagnetic data: Tectonophysics, v. 184, p. 1–9, doi:10.1016/0040-1951(90)90116-P.

van Hinsbergen, D.J.J., and Schmid, S.M., 2012, Map view restoration of Aegean–west Anatolian accretion and extension since the Eocene: Tectonics, v. 31, no. 5, doi:10.1029/2012TC003132.

Early Cretaceous–present latitude of the proto-Tibetan Plateau

van Hinsbergen, D.J.J., Kapp, P., Dupont-Nivet, G., Lippert, P.C., DeCelles, P.G., and Torsvik, T.H., 2011a, Restoration of Cenozoic deformation in Asia and the size of Greater India: Tectonics, v. 30, TC5003, doi:10.1029/2011TC002908.

van Hinsbergen, D.J.J., Steinberger, B., Doubrovine, P.V., and Gassmöller, R., 2011b, Acceleration-deceleration cycles in India-Asia convergence: Roles of mantle plumes and continental collision: Journal of Geophysical Research, v. 116, B06101, doi:10.1029/2010JB008051.

van Hinsbergen, D.J.J., Lippert, P.C., Dupont-Nivet, G., Kapp, P., DeCelles, P.G., and Torsvik, T.H., 2012a, Restoration of Cenozoic deformation in Asia, and the size of Greater India: Reply: Tectonics, v. 31, p. TC4007, doi:10.1029/2012TC003144.

van Hinsbergen, D.J.J., Lippert, P.C., Dupont-Nivet, G., McQuarrie, N., Doubrovine, P.V., Spakman, W., and Torsvik, T.H., 2012b, Greater India Basin hypothesis and a two-stage Cenozoic collision between India and Asia: National Academy of Sciences Proceedings, v. 109, p. 7659–7664, doi:10.1073/pnas.1117262109.

van Hinsbergen, D.J.J., Vissers, R.L.M., and Spakman, W., 2014, Origin and consequences of western Mediterranean subduction, rollback, and slab segmentation: Tectonics, v. 33, p. 393–419, doi:10.1002/tect.20125.

Volkmer, J.E., Kapp, P., Guynn, J.H., and Lai, Q.Z., 2007, Cretaceous–Tertiary structural evolution of the north central Lhasa terrane, Tibet: Tectonics, v. 26, TC6007, doi:10.1029/2005TC001832.

von der Heydt, A., and Dijkstra, H.A., 2008, The effect of gateways on ocean circulation patterns in the Cenozoic: Global and Planetary Change, v. 62, p. 132–146, doi:10.1016/j.gloplacha.2007.11.006.

Wallace, J.M., and Hobbs, P.V., 2006, Atmospheric Science: An Introductory Survey (second edition): Amsterdam, Elsevier, 483 p.

Wang, C.S., Zhao, X.X., Liu, Z.F., Lippert, P.C., Graham, S.A., Coe, R.S., Yi, H., Zhu, L., Liu, S., and Li, Y., 2008, Constraints on the early uplift history of the Tibetan plateau: National Academy of Sciences Proceedings, v. 105, p. 4987–4992, doi:10.1073/pnas.0703595105.

Wang, E., Kirby, E., Furlong, K.P., van Soest, M., Xu, G., Shi, X., Kamp, P.J., and Hodges, K.V., 2012, Two-phase growth of high topography in eastern Tibet during the Cenozoic: Nature Geoscience, v. 5, p. 640–645, doi:10.1038/ngeo1538.

Wang, J., Hu, X., Jansa, L., and Huang, Z., 2011, Provenance of the Upper Cretaceous–Eocene deep-water sandstones in Sangdanlin, southern Tibet: Constraints on the timing of initial India-Asia collision: Journal of Geology, v. 119, p. 293–309, doi:10.1086/659145.

Westphal, M., and Pozzi, J.P., 1983, Paleomagnetic and plate tectonic constraints on the movement of Tibet: Tectonophysics, v. 98, p. 1–10, doi:10.1016/0040-1951(83)90207-X.

Westphal, M., Pozzi, J.-P., Zhou, Y.X., Xing, L.S., and Chen, X.Y., 1983, Palaeomagnetic data about southern Tibet (Xizang)—I. The Cretaceous formations of the Lhasa block: Royal Astronomical Society Geophysical Journal, v. 73, p. 507–521, doi:10.1111/j.1365-246X.1983.tb03327.x.

Wiesmayr, G., and Grasemann, B., 2002, Eohimalayan fold and thrust belt: Implications for the geodynamic evolution of the NW-Himalaya (India): Tectonics, v. 21, 1058, doi:10.1029/2002TC001363.

Yan, D.-P., Zhou, M.-F., Li, S.-B., and Wei, G.-Q., 2011, Structural and geochronological constraints on the Mesozoic–Cenozoic tectonic evolution of the Longmen Shan thrust belt, eastern Tibetan Plateau: Tectonics, v. 30, TC6005, doi:10.1029/2011TC002867.

Yan, M.D., Van der Voo, R., Tauxe, L., Fang, X.M., and Pares, J.M., 2005, Shallow bias in Neogene palaeomagnetic directions from the Guide Basin, NE Tibet, caused by inclination error: Geophysical Journal International, v. 163, p. 944–948, doi:10.1111/j.1365-246X.2005.02802.x.

Yi, Z., Huang, B., Chen, J., Chen, L., and Wang, H., 2011, Paleomagnetism of early Paleogene marine sediments in southern Tibet, China: Implications to onset of the India-Asia collision and size of Greater India: Earth and Planetary Science Letters, v. 309, p. 153–165, doi:10.1016/j.epsl.2011.07.001.

Yin, A., Harrison, T.M., Ryerson, F.J., Chen, W.J., Kidd, W.S.F., and Copeland, P., 1994, Tertiary structural evolution of the Gangdese thrust system, southeastern Tibet: Journal of Geophysical Research, v. 99, p. 18175–18201, doi:10.1029/94JB00504.

Yue, Y.H., and Ding, L., 2006, ^{40}Ar/^{39}Ar geochronology, geochemical characteristics and genesis of the Linzhou basic dikes, Tibet: Acta Petrolei Sinica, v. 22, p. 855–866.

Zhang, K.J., 2000, Cretaceous palaeogeography of Tibet and adjacent areas (China): Tectonic implications: Cretaceous Research, v. 21, p. 23–33, doi:10.1006/cres.2000.0199.

Zhang, Z., Nisancioglu, K.H., Flatoy, F., Bentsen, M., Bethke, I., and Wang, H., 2011, Tropical seaways played a more important role than high latitude seaways in Cenozoic cooling: Climate of the Past, v. 7, p. 801–813, doi:10.5194/cp-7-801-2011.

Zhu, D.-C., Mo, X.-X., Niu, Y., Zhao, Z.-D., Wang, L.-Q., Liu, Y.-S., and Wu, F.Y., 2009, Geochemical investigation of Early Cretaceous igneous rocks along an east-west traverse throughout the central Lhasa Terrane, Tibet: Chemical Geology, v. 268, p. 298–312, doi:10.1016/j.chemgeo.2009.09.008.

Zhu, Z., Zhu, X., and Zhang, Y., 1981, Paleomagnetic observation in Xizang (Tibet) and continental drift: Acta Geologica Sinica, v. 24, p. 40–49.

Zhuang, G.S., Hourigan, J.K., Ritts, B.D., and Kent-Corson, M.L., 2011, Cenozoic multiple-phase tectonic evolution of the northern Tibetan plateau: Constraints from sedimentary records from Qaidam basin, Hexi corridor, and Subei basin, northwest China: American Journal of Science, v. 311, p. 116–152, doi:10.2475/02.2011.02.